Bioorganic Chemistry 105 (2020) 104358

Contents lists available at ScienceDirect

Bioorganic Chemistry

journal homepage: www.elsevier.com/locate/bioorg

Design, synthesis and molecular modeling studies of 2-styrylquinazoline derivatives as EGFR inhibitors and apoptosis inducers

Noha H. Amin [a,*], Mohammed T. Elsaadi [a,b], Shimaa S. Zaki [a], Hamdy M. Abdel-Rahman [c,d]

[a] Department of Medicinal Chemistry, Faculty of Pharmacy, Beni-Suef University, Beni-Suef 62514, Egypt
[b] Department of Medicinal Chemistry, Faculty of Pharmacy, Sinai University-Kantra Branch, Egypt
[c] Department of Pharmaceutical Chemistry, Faculty of Pharmacy, Nahda University, Beni-Suef, Egypt
[d] Department of Medicinal Chemistry, Faculty of Pharmacy, Assiut University, 71526 Assiut, Egypt

ARTICLE INFO

Keywords:
Quinazoline
Styryl
Sulfonamide
Antitumor
EGFR inhibition
Molecular docking

ABSTRACT

Herein, we report the synthesis of novel 2-substituted styrylquinazolines conjugated with aniline or sulfonamide moieties, anticipated to act as potent anticancer therapeutic agents through preferential EGFR inhibition. In doing so, all the synthesized compounds were screened for their *in vitro* anticancer activities (nine subpanels) at the National Cancer Institute (NCI), USA. The resulting two most active anticancer compounds (**7b** and **8c)** were then chemically manipulated to investigate feasible derivatives (**12a-e** and **15a-d**). MTT cytotoxicity, *in vitro* cell free EGFR and anti-proliferative activity against EGFR/ A549 cell line evaluation for the most active broadly spectrum candidates (**7a/b**, **8c/e**, **12b** and **15d**) was conducted. Promising results were obtained for the styrylquinazoline-benzenesulfonamide derivative **8c** (IC_{50} = 8.62 μM, 0.190 μM and = 79.25%), if compared to lapatanib (IC_{50} = 11.98 μM, 0.190 μM, and 79.25%), respectively. Moreover, its apoptotic induction potential was studied through cell cycle analysis, Annexin-V and caspase-3 activation assays. Results showed a clear cell arrest at G2/M phase, a late apoptotic increase (76 folds) and a fruitful caspase-3 expression change (8 folds), compared to the control. Finally, molecular docking studies of compounds **7a/b, 8c/e, 12b** and **15d** revealed proper fitting into the active site of EGFR with a low binding energy score for compound **8c** (−13.19 Kcal/mole), compared to lapatanib (−14.54 Kcal/mole).

1. Introduction

Cancer has been classified as one of the leading life-threatening causes worldwide owing to its massive and complicated etiology [1]. That is not to mention the therapeutic struggle against lack of selectivity and safety, ongoing resistance emergence and various side effects of anticancer drugs, even of those that have been already approved by Food and Drug Administration (FDA). Accordingly, vital needs for developing and discovering potent and selective anticancer agents have never ceased or has their importance been lessened. [2]. Anti-neoplastic chemotherapeutic development has passed through several stages starting from using non-specific cytotoxic agents to more specified and even multi-targeted agents that modulated vital cell proteins including different kinases [3]. Protein tyrosine kinases (PTKs) have been identified as essential cellular enzymes that regulate proliferation, differentiation and apoptosis [4]. PTKs have been responsible for the phosphorylation catalysis of tyrosine or serine/threonine residues of various regulatory proteins [5]. They can be chiefly classified into either receptor such as epidermal growth factor receptor (EGFR) kinases or non-receptor ones such as B-RAF. However, EGFR-TK is considered the prototype of the EGFR (ERBB, class I RTK) family that has been identified as a trans membrane receptor tyrosine kinase belonging to ErbB family [6], where its overexpression has been found to be abundant in a number of various cancers such as non-small cell lung cancer (NSCLC), head and neck cancer, breast cancer and colorectal cancer [7-10]. Accordingly, the inhibition of tyrosine kinase activity has provided a rational approach to cancer therapy through the discovery of totally newly synthesized anti-neoplastic compounds or the structural manipulations of already known molecular cores [11].

A wide range of structural compounds have been reported to act as

Abbreviations: NCI, National Cancer Institute; RTKs, receptor tyrosine kinases; EGFR, epidermal growth factor receptor; MTT, 3-2(4,5-dimethylthiazol-2-yl)-2,5-diphenyltetrazolium bromide dye compound; SEM, standard error of the mean.

* Corresponding author.
E-mail address: noha.metri@pharm.bsu.edu.eg (N.H. Amin).

https://doi.org/10.1016/j.bioorg.2020.104358
Received 6 July 2020; Received in revised form 5 September 2020; Accepted 5 October 2020
Available online 8 October 2020

potent EGFR inhibitors, notably compounds containing a quinazoline ring, the ring which has a well-known historical wide range of therapeutic efficacy as bioactive antitumor [12-14], analgesic, anti-inflammatory [15], antifungal [16], antibacterial [17,18] or antiviral agents [19]. Interestingly, several FDA approved antitumor agents that may act as EGFR inhibitors shared the possession of a quinazoline core. Further exploration of such cores demonstrated the importance of specific quinazoline derivatives over others, namely 4-anilinoquinazoline derivatives, such as the FDA approved geftinib and erlotinib [20]. However, mutation related resistance has always been a problem to face and was successfully overcome though developing a second generation of irreversible covalently bound EGFR inhibitors, such as afatinib, which in turn led to several dose limiting toxicities in the clinical filed ranging from skin rash and up to kidney failure [21]. Accordingly and despite of the arising numbers of such therapeutic agents, the consistent necessity for a continuous flow of EGFR inhibitors development has been practically confirmed to catch up with any arising irreversibility, selectivity or toxicity obstacles [20,21]. Recapturing variant antitumor potencies of the quinazoline moiety through EGFR inhibition, remarkable antiproliferative activities and other multiple mechanisms against various cancerous cell lines, in accordance with its accessible chemistry manipulation in the laboratory, roused scientists to invest in such a molecule [6,22].

In the same direction, it has been expected that the quinazoline ring can still present a wide range of versatile chemical and biological outcomes to humanity. Accordingly, the present research was based on the chemical covalent hybridization of the quinazoline ring at different positions with other structurally chemical moieties of known effective anticancer activities in order to augment the overall pharmacological antitumor outcome of such hybrids, anticipated to exert their action through EGFR inhibition.

2. Rationale and design

Literature survey of several potent FDA approved EGFR inhibitors has been investigated and subsequently correlated to clinical trials. Observations were taken and it was concluded that 4-anilinoquinazoline derivatives, such as gefitinib **A** (IC_{50} = 0.090 μM), erlotinib **B** (IC_{50} = 0.025 μM) and lapatinib **C** (IC_{50} = 0.115 μM), have been valuable commodities for further exploration as anticancer agents [6,20-22].

On the other hand, the power of sulfonyl/ sulfonamide has been fruitfully explored for their efficacy and considerable safety margins as anti-tumor agents [23]. Introduction of a sulfonamide functionality onto various heterocyclic nuclei has produced candidates with a clear antitumor activity spring over the sulfonamide free ones [24].

Nevertheless, bioisosteric quinolone and quinazoline-benzenesulfonamide hybrids have been investigated throughout literature as potent EGFR inhibitors against various cancerous cell lines [12]. Promising antitumor activity results were obtained throughout various literature studies demonstrated by quinazoline derivatives bearing a sulfonamide moiety (IC_{50} values in the nanomolar range against MCF-7) [25,26]. One prominent example was compound D, the most potent amongst a series of tested compounds (IC50 = 0.13 nmol). Its mechanism of action was illustrated via molecular modelling, where it showed a similar binding mode to that of geftinib and lapatinib at EGFR tyrosine kinase binding site. It acted via competing with ATP for binding at the catalytic domain of EGFR tyrosine kinase [11].

Meanwhile, the worldwide immune stimulatory chloroquine (4-anlinoquinoline skeleton) has aroused increasing attention owing to its antiproliferative potency and excellent antiangiogenesis activities against different types of cancer. Furthermore, some 2-substituted-4-anilinoquinoline derivatives (2-arylsufonyl/ styrylquinolone) were synthesized and evaluated for their antiproliferative activity against four human cancerous cell lines, where highly improved anticancer activities were noticed for 2-styrylquinolone derivatives over other analogues. Also, it was observed that the introduction of a suitable spacer (ethylene linkage) between the quinolone nucleus and the aryl moiety resulted in a considerable antitumor activity upgrade, exemplified by compound **E** (2-methoxystyryl quinolone) [27-29]. Compound **E** has shown significant *in vitro* antiproliferative activity against lung, colon, liver and gastric cancerous cell lines (IC_{50} = 0.03 μM, 0.55 μM, 0.33 μM and 1.24 μM against H-460, HT-29, HepG2 and SGC-7901 cell lines, respectively), reaching up to 186 folds more active than gefitinib. Accordingly, such quimoline derivatives could be considered as promising scaffolds for producing effective antitumor candidates through further structural modifications and/ or using other bioisosteric congeners such as quinazolines [28,29].

Wrapping up the above mentioned scientific literature results, the present research work proposed a schematic outline for the design and synthesis of novel quinazoline hybrids **(series 7, 8, 12 and 15).** The present quinazoline scaffolds have been synthesized through an effective covalent hybridization technique between a 4-substituted styrylquinazoline backbone with various substituted aniline/ sulfonamide moieties at position 4 of the intended quinazoline, hoping to augment the overall molecular antitumor activity of the resulting hybrids (**7a-e** and **8a-e**).Those newly synthesized hybrids have been expected to act as potent anticancer therapeutic agents through EGFR inhibitory activities owing to the quinazoline nitrogenous moiety presence, capable of forming H-bonds with the hinge region of EGFR active site, and thus resembling the ATP binding site of EGFR. Generation of such novel chemical hybridized entities has been predicted to demonstrate arising hydrophobic interaction with the ATP-binding site of EGFR at various sites. Moreover, bulky substituted aniline/ sulfonamide moieties at C4 of quinazoline have been expected to serve as an easily reachable lyophilic part for the rear side of the ATP binding site and thus offering a more stable and comfortable positioning**.** Alongside the C-4 quinazoline substitution, another C-2 quinazoline substitution with a methoxyphenyl moiety was performed using the previously reported promising spacer (ethylene linkage), Fig. 1**.**

Additionally, the resulting most active antitumor candidates **(7b** and **8c)** have been substituted with a variety of structural styryl side chains to investigate feasible pharmacological outcomes of such chemical structural derivatives (**12** and **15**). Furthermore, evaluation of the antitumor activity of the synthesized compounds against a panel of cancerous cell lines, EGFR screening assay, in addition to their ability to induce apoptosis and cell cycle analysis, were also performed. It has been conceptualized that the resulting pharmacophoric figure would act as a promising template for potent anticancer agents with acceptable safety margins through EGFR inhibition**,** Fig. 2**.**

3. Results and discussion

3.1. Chemistry

The target compounds were synthesized according to the depicted Schemes 1-3. The structures of the newly synthesized compounds were established on their elemental analyses and spectral data (Supplementary). As a starting point in Scheme 1**,** the 2-methylquinazolin-4(3H)-one nucleus **3** was synthesized following Niementowski synthesis through the direct anhydrous fusion of anthranilic acid **1** with thioacetamide **2** in a molar ratio of 1: 1.5 [30]. Then compound **3** was used as the main synthetic backbone for the newly synthesized target compounds **7a-e** and **8a-e.** The key intermediates **5** and **6** were prepared through the reaction of 2-methylquinazolin-4(3H)-one **3** with p-methoxybenzaldehyde **4** in acetic acid to afford 2-methylquinazolin-4 (3H)-one **5**, followed by its chlorination reaction with phosphorus oxychloride in ether to result in 4-chloro-2-methylquinazoline **6** under controlled conditions of temperature and time [31]. Furthermore, the target compounds **7a-e** were synthesized through the condensation reaction of the building block, 4-chloro-2-(4-methoxystyryl) quinazoline **6,** with different amines in DMF in presence of potassium carbonate, except for compounds **7a** and **7c** that were stirred in isopropanol and

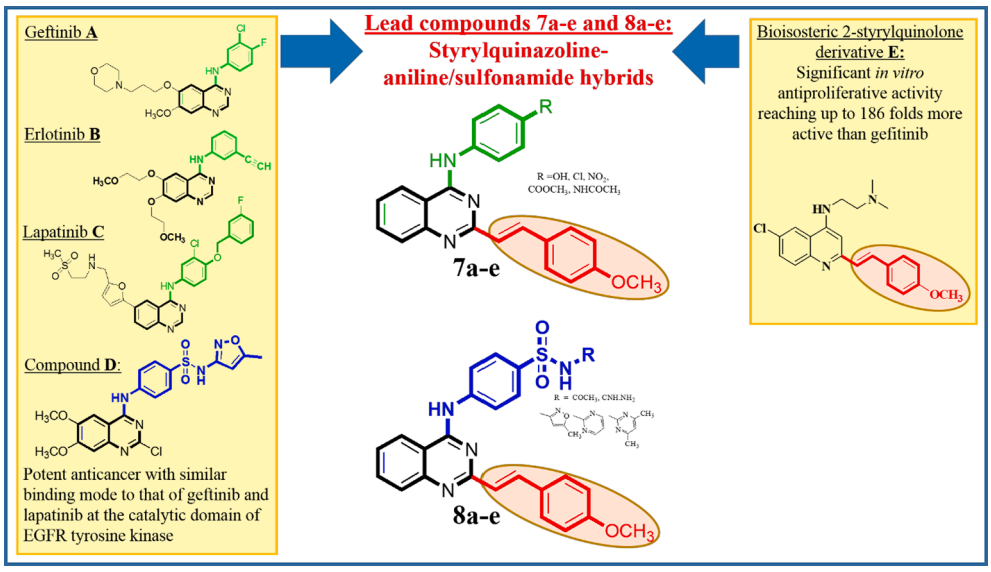

Fig. 1. Design strategy of the present compounds **7a-e** and **8a-e.**

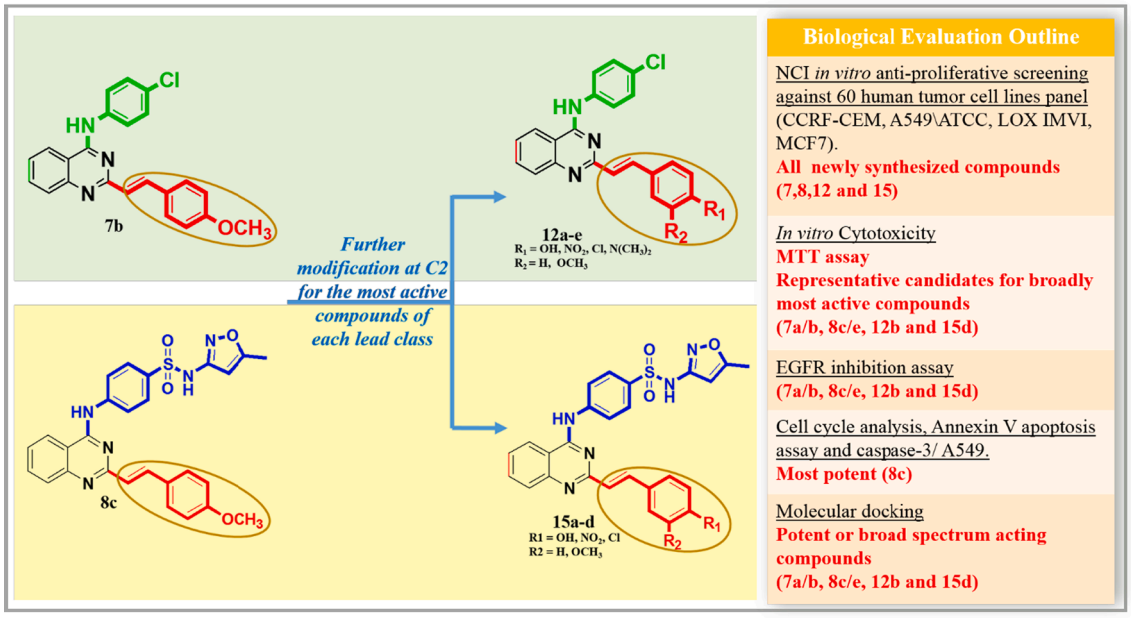

Fig. 2. Chemical modifications of the most active candidates **7b** and **8c** and further biological evaluation.

ethylene glycol, respectively. Similarly, condensing 4-chloro-2-(4-methoxystyryl) quinazoline **6** with different sulfonamides in absolute ethanol in presence of anhydrous potassium carbonate, as a suitable acid eliminating reagent, afforded sulfonyl derivatives **8a-e** in good yields.

In Scheme 2, Endicot modified synthetic method was adopted to obtain the key intermediate, 4-chloro-2-methylquinazoline **9** through keeping temperature and work-up time to minimum and immediately purifying the crude in neutral medium in order to avoid any possible instability of 4-chloroquinazoline to an acid**.** The synthesis was conducted through the activation of position 4 of 2-methylquinazolin-4 (3H)-one **3** by chlorination with phosphorus oxychloride at minimum temperature for minimum time [32] and then followed by a condensation reaction with p-chloroaniline **10** in DMF in presence of potassium carbonate to afford N-(4-chlorophenyl)-2-methylquinazolin-4-amine **11**. Moreover, the target substituted styryl derivatives **12a-e** were synthesized through the reaction of appropriate substituted aldehydes with compound **11** in glacial acetic acid in presence of sodium acetate under classical condensation conditions of appropriate aldehydic dervitisation.

Furthermore in Scheme 3**,** N-(5-methylisoxazol-3-yl)-4-((2-methylquinazolin-4-yl)amino) benzenesulfonamide **14,** another key intermediate that was prepared through the reaction of 4-chloro-2-methylquinazoline **9** with sulfamethoxazole **13** in ethanol in presence of anhydrous potassium carbonate. Last but not least, the target compounds **15a-e** were prepared through a condensation reaction of compound **14** with different aldehydes in glacial acetic acid in presence of sodium acetate.

3.2. *In vitro cytotoxic screening and SAR discussion*

The obtained screening results of all the present newly synthesized compounds were obtained from the National Cancer Institute (NCI), Bethesda, Maryland, USA, represented as mean graph of the percent growth of treated cells (Supplementary **tables S1 and S2**) and then demonstrated as percent of growth inhibition (GI %) in Figs. 3a and 3b

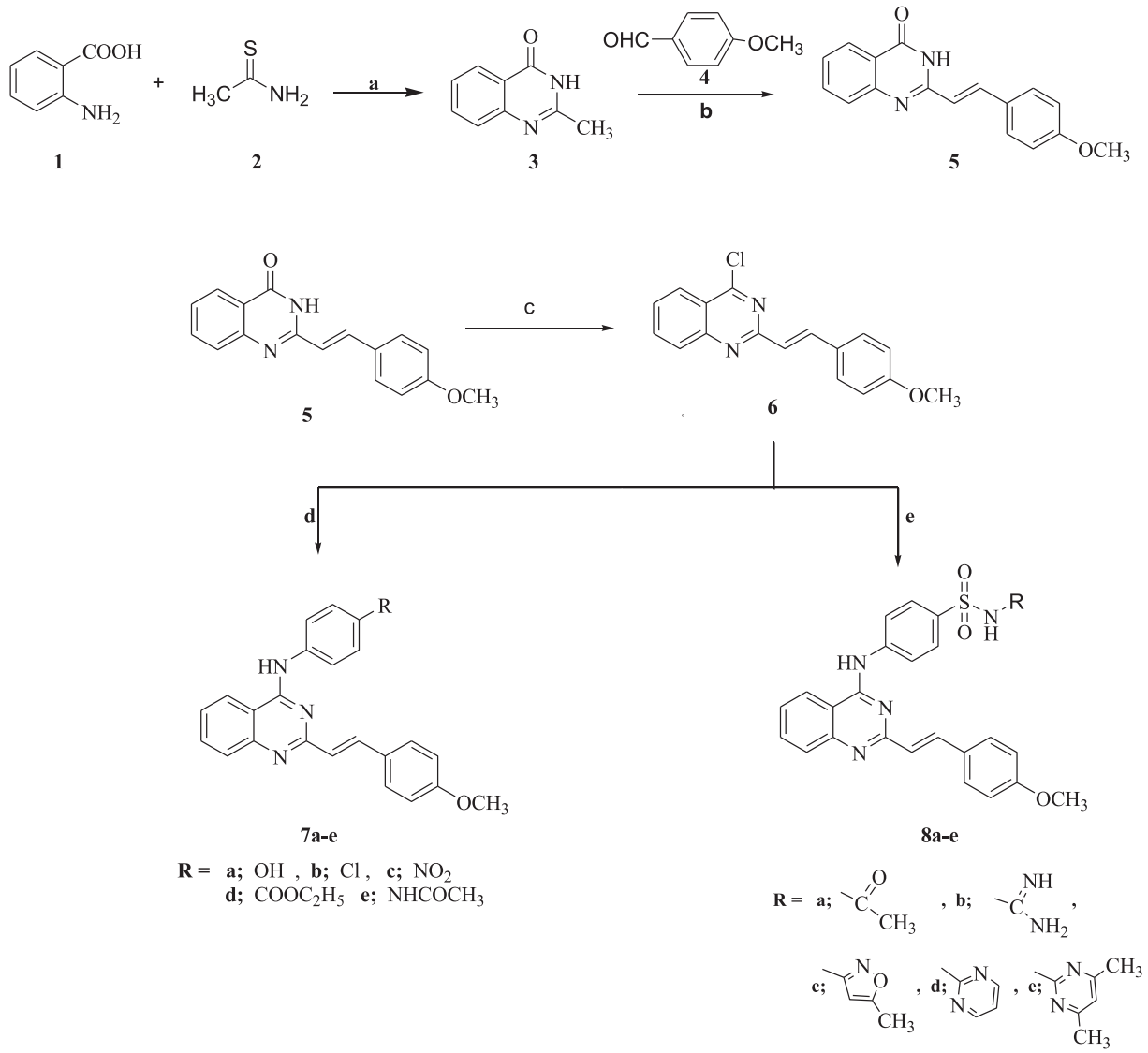

Scheme 1. Synthesis of compounds **3, 5, 6,7a-e** and **8a-e. Reagents and reaction conditions: a.** Reflux, 2 h; **b.** Acetic acid, Na acetate, reflux, 24 h; **c.** $POCl_3$, reflux, 2 h; **d.** Appropriate amine, DMF/ K_2CO_3 or isopropanol or ethylene glycol, reflux, 24 h; **e.** Appropriate sulfonamide, ethanol, K_2CO_3, reflux, 24 h.

[33-35]. The obtained results showed that the tested quinazoline derivatives possessed a broad-spectrum anti-tumor activity, particularly against non-small cell lung cancer A549\ ATCC and breast cancer MCF7 (known for EGFR over expression), ranging from GI % = 64.79 to 20.21% and from GI % = 69.32 to 21.55%, respectively.

It was observed that the tested quinazoline derivatives exhibited a distinctive pattern of selectivity. Leukemia CCRF-CEM cell lines were found to be remarkably sensitive to compounds **7a** and **7b** (GI % = 87.14 and 91.94%, respectively). In addition, leukemia TB cell lines showed sensitivity to compound **7a (**GI % = 89.9%). Also, compounds **8c** and **8e** exhibited considerable activities against leukemia SR cells (GI % = 54.57 and 50.53%, respectively).

Regarding non-small lung cancer, A549\ATCC cell lines showed sensitivity towards a variety of compounds such as **7b** and **8a,c,e** (GI % = 64.97, 57.99, 60.86 and 57.75%, respectively). Also, NCI-H322M cell lines were sensitive to compounds **7b** and **8a,c,e** (GI % = 55.73, 61.39, 62.66 and 70.98%). Additionally, strong anticancer activities of compounds **7b** and **7a** against NCI-H460 and NCI-H522 cell lines were recorded (GI % = 81.8 and 84.74%, respectively).

In respect to melanoma, LOX IMVI cell line, diverse compounds showed various activities such as **7b** and **8a,c,e (**GI % = 81.63, 61.71, 68.53 and 73.69%, respectively). UACC-62 cell line displayed sensitivity to compounds **7b,c** and **8a,c,e** (GI % = 85.68, 63.74, 74.4, 82.48 and 79.18%, respectively).

Concerning renal cancer, A498 cell lines presented powerful sensitivity against compounds **7b,e** and **8a,c,e (**GI % = 83.37, 90.34, 90.42, 98.27 and 92.2%, respectively).

Moreover, Breast cancer, MCF7 cell lines proved to be sensitive to compounds **7b** and **8a,c,e** (GI % = 55.99, 53.34, 67.92 and 57.84%, respectively), while MDA-MB-468 cell lines showed moderate sensitivity to compounds **7b** and **8c,e** (GI % = 71.92, 70.06 and 75.98%, respectively).

In an attempt to discover more anti-tumor active agents, compounds **7b** and **8c** were used as lead compounds and were selected for further derivativization by different aldehydic compounds at position two to give series **12a-e** and **15a-d,** which were later screened also at NCI and the results obtained were demonstrated as percent of inhibition. (Supplementary; table 2**s**)

Unfortunately, compound **15d** showed remarkably low cell growth promotion against melanoma MDA-MB-435 cell line (GI % = −44.14%), but on the other hand it demonstrated a broad spectrum activity against leukemia K-562, SR cell lines (GI % = 82.21 and 80.58%, respectively), colon cancer HCT-15, KM12 (GI % = 68.24 and 68.22%, respectively) and breast cancers MCF7 (GI % = 69.32%). Also, compounds **12b,d** and

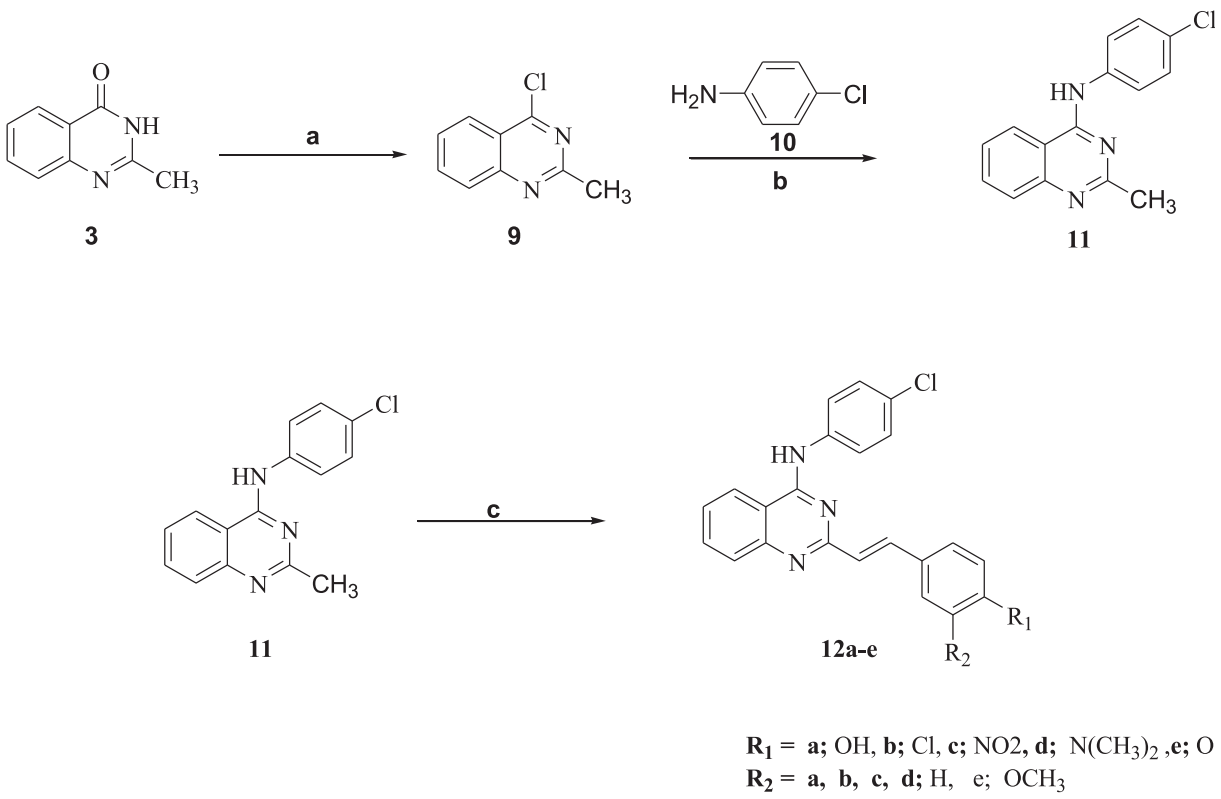

Scheme 2. Synthesis of compounds **9, 11** and **12a-e. Reagents and reaction conditions: a.** $POCl_3$, reflux, 2 h; **b.** DMF, K_2CO_3, reflux, 24 h; **c.** Appropriate aldehyde, glacial acetic acid, Na acetate, reflux, 24 h.

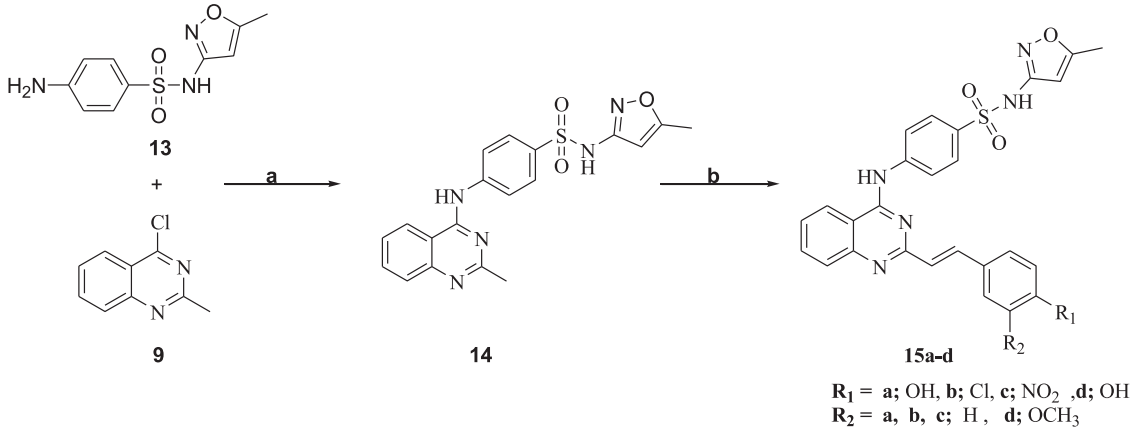

Scheme 3. Synthesis of compounds **14** and **15a-d. Reagents and reaction conditions: a.** Ethanol, anhydrous K_2CO_3, reflux, 24 h; **b.** Appropriate aldehyde, glacial acetic acid, Na acetate, reflux, 24 h.

15b exhibited moderate anti-tumor activity against leukemia (K-562 and SR cell lines), melanoma (LOX IMVI and UACC-62) and breast cancers (MCF7).

Structure activity results correlation was based on several literature reviews about effective EGFR inhibitors, where these compounds compete with ATP for binding with the catalytic domain of tyrosine kinase, exemplified by quinazoline cores, especially those substituted at position 4 like the reference drug, lapatinib. It has been noticed that such cores effectively bind with ATP binding cleft through hydrophobic interactions with hydrophobic pocket in *N*-terminal domain of EGFR enzyme via its two nitrogen atoms, acting as hydrogen bond acceptors. Similarly, the present newly synthesized quinazoline hybrids that were substituted with aniline/sulfonamide moieties at C-4 and variable substituted styryl moieties at C-2 were expected to interact at the same position as 3-chloro-4-(3-fluorobenzyl)oxy moiety of lapatinib, where such lipophyllic substitutions should lead to better fitting into the EGFR binding site. Accordingly, the present synthesized compounds were expected to act similarly and was practically demonstrated via their significant GI% against variable cell lines, such as the quinazoline hybrids between substituted aniline moieties at C-4 and methoxystyryl at C-2, exemplified by compounds **7a** (GI % = 89.9%) and **7b** (GI % = 91.94%) against leukemia cell lines (CCRF-CEM and TB). Similarly, the quinazoline hybrids between benzenesaulfonamide moities at C-4 and methoxystyryl at C-2, exemplified by compounds **8c** (GI % = 98.27%) and **8e** (GI % = 92.2%) showed considerable anticancer activities against renal cancer cell lines (A498) [11]. Furthermore, variable substituents have been incorporated on the aniline/ sulfonamide of C-4 and styryl of C-2 moieties of the quinazoline ring to investigate their

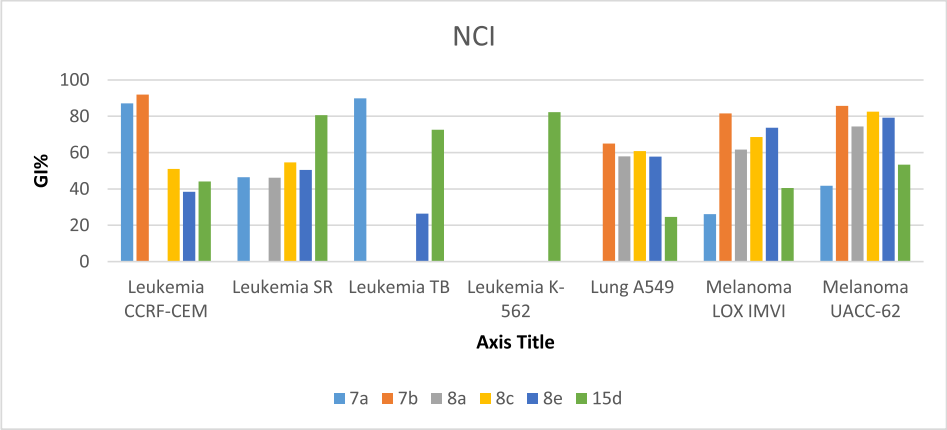

Fig. 3a. GI % of compounds **7a**, **7b**, **8a, 8c, 8e** and **15d** over the most sensitive cell lines (Leukemia, lung and melanoma subpanels).

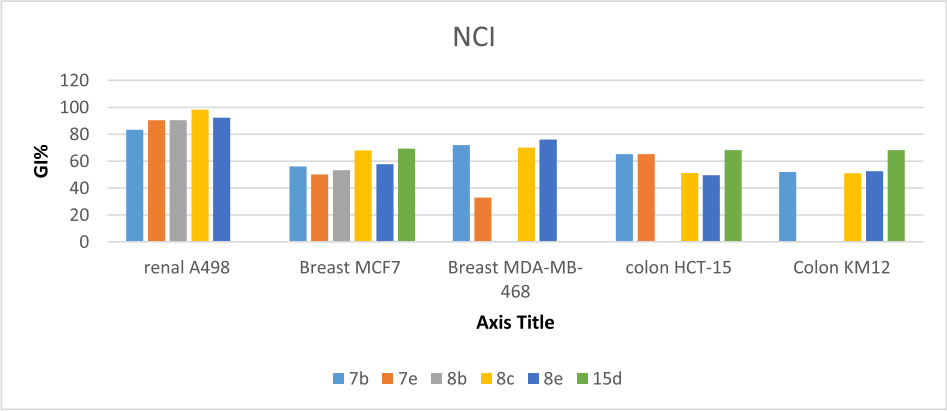

Fig. 3b. GI % of compounds **7a**, **7b**, **8a, 8c, 8e** and **15d** over the most sensitive cell lines (Renal, breast and colon subpanels).

influence on pharmacological activity. Generally 2-substituted methoxystyryl qunazoline derivatives **7a** (hydroxyaniline), **7b** (chloroaniline), **8c** (isoxazolyl benzenesulfonamide) and **8e** (dimethylpyrimidine) have proved a dramatic activity improvement over other non methoxystyryl quinazoline derivatives such as compounds **12b (**chlorostyryl) or **12d (**dimethylaminoatyryl) derivatives. However, compound **15d** was an exception as it was a methoxystyryl derivative that showed a remarkably low GI % = −44.14 against melanoma (MDA-MB-435) subpanel.

3.3. Cytotoxicity potential assay study

3.3.1. Cytotoxicity potential assay study (MTT assay)

Representative most active compounds showing broad spectrum activity (**7a, 7b, 8c, 82, 12b** and **15d)** were selected to be further tested for their cytotoxicity potency using MTT test and results were expressed as $IC_{50\%}$, Table 1 and Fig. 4**.** Non-small cell lung cancer cell lines (A549, obtained from the American Type Culture Collection, Rockville, MD, USA) were chosen for the assay for their well-known fact of EGFR overexpression [36]. Interestingly, 2,4-disubstituted quinazoline derivative **8c** (IC_{50} = 8.62 μM) showed potent cytotoxicity against A549 cell line, almost double that of lapatinib (IC_{50} = 11.98 μM). On the other hand, moderate activity was shown by compounds **7a, 8e** and **15d** (nearly reaching half that of lapatinib), while compounds **7b** and **12b** possessed the lowest anti-tumor activity. These findings have been attributed to the presence of both the methoxystyryl group and the oxazolyl moiety as a sulphonamide derivative rather than any other substitution at position 4. Also, a general positive effect of the lipophilic impact of such derivatives upon interacting with EGFR active binding site has been expected to contribute in their relative overall antitumor effects as shown by log P values, Table 1. Moreover, MTT IC_{50} values and selectivity index (SI) for the same compounds were performed on normal lung fibroblasts (WI38), noncancerous cell lines used as a reference to check for a possible tumor selectivity and thus expected toxicity**.** Compounds **7b, 8e** and **12b** showed good selectivity results (less than 1), even better than those of lapatinib, so proving greater safety margins. On the other hand, compounds **7a, 8c** and **15d** showed mild to moderate toxicity (SI more than one and less than 25), Table 1**.**

Table 1
Cytotoxicity assay (MTT) and log P values of compounds **7a, 7b, 8c, 8e, 12b** and **15 d** and lapatanib against non-small lung cancer cell lines (A549) and normal lung fibroblasts (WI38).

Compound ID	IC_{50} [a] (μM) (Mean ± SEM) [b]		SI [(c)]	CLog P
	A549	WI38		
7a	26.69 ± 1.60	65.5 ± 3.68	1<	5.81
7b	31.35 ± 1.80	28.4 ± 1.6	1>	7.22
8c	8.62 ± 0.50	52.6 ± 2.95	1 <	5.81
8e	28.85 ± 1.70	27.3 ± 1.53	1>	6.35
12b	43.38 ± 2.50	18.1 ± 1.02	1>	8.01
15d	27.98 ± 1.60	45.0 ± 2.53	1 <	5.08
Lapatinib	11.98 ± 0.70	17.0 ± 0.96	1 <	NT[(d)]

(a): IC_{50} values are the mean of three separate experiments and is a concentration that causes 50% growth inhibition, (b): Standard error of the mean, Values are the mean ± SD (n = 3).
(c): SI = Selectivity Index = IC_{50} value normal cell/IC_{50} value cancer cell.
(d): Not tested.

Table 2
IC50 values and growth inhibition percent of target compounds **7a, 7b, 8c, 82, 12b** and **15 d** and lapatinib against EGFR.

Compound ID	EGFR	
	% Inhibition at 1 μg/ml	IC_{50} [a] (μM) (Mean ± SEM) [b]
7a	63.49	0.355 ± 10.15
7b	62.58	0.369 ± 10.50
8c	69.71	0.190 ± 5.44
8e	62.70	0.307 ± 8.79
12b	66.05	0.269 ± 7.70
15d	60.86	0.634 ± 18.11
Lapatinib	75.09	0.115 ± 0.003
Control	NT[c]	NT

(a): IC_{50} values are the mean of five separate experiments and is a concentration that causes 50% growth inhibition, (b): Standard error of the mean, (c): not tested.

3.4. Epidermal growth factor receptor enzyme inhibition assay

3.4.1. In vitro EGFR enzyme inhibition assay

A further EGFR kinase assay was carried out against A549 cell lines, known for their EGFR overexpression, to study the postulated mechanism of action of the present synthesized compounds. With reference to the preceding considerable antiproliferative screening results against 60 cell lines and expressive cytotoxicity results, compounds **7a** (p-hydroxyphenyl derivative) and **7b** (*para*-chloro phenyl derivative) for aniline-methoxystyrylquinazolines**, 8c** (methylisoxazole derivative) and **8e** (dimethyl pyrimidine) for sulfonamide–methoxystyrylquinazoline, in addition to compounds **12b** and **15d** were all subjected to *in vitro* cell free EGFR enzyme inhibition determination using EnzyChromTM Kinase Assay Kit (EKIN-400) according to manufacturer's instructions by ELISA assay method and using lapatinib as a reference [36,37]. Table 2 and Fig. 4**.**

The obtained results that compound **8c** exhibited showed potent inhibition of EGFR enzyme (IC_{50} = 0.190 μM) if compared to lapatinib (EGFR IC_{50} = 0.115 μM). This inhibitory activity was attributed to the presence of a p-methoxystyryl moiety as previously mentioned, in addition to the oxazole ring of sulphonamide moiety. Furthermore, compounds **7a, 7b, 8e** and **12b** showed moderate EGFR inhibition. Also, it could be concluded that the sulfonamide derivative **8e** was favored over other substituted aniline derivatives in position 4 (**7a, 7b**). Moreover, compounds **15d** possessed low EGFR inhibition activity when the methoxy group was changed to a chloro moiety.

3.4.2. In vitro EGFR enzyme inhibition assay of target compounds against EGFR-expressed in A549 cell line

Further investigation was performed for the compounds **7a, 7b, 8c, 8e**, **12b** and **15d,** which showed good antitumor activity results against EGFR enzyme, using a more specific expressed EGFR activity in A549 cell line at confirmatory diagnostic unit at VACSERA, Cairo [37]. NSCLC cell lines (A549) were treated with the desired compounds with their IC_{50} concentrations for accurate assay then lysed and subjected to enzyme-linked-immunosorbent assay (ELISA) to determine their activity against EGFR in this cell line. The results were presented as percentage inhibition. The results were consistent with *in vitro* EGFR assay, which also showed expected high potency of compound **8c** (% inhibition of EGFR enzyme in cell line A549 = 79.25%) and that was pretty comparable to that of lapatinib (83.33%). These findings confirmed the importance of p-methoxystyryl moiety for EGFR inhibition**.** On the other hand, moderate activity was presented by compounds **7a, 7b, 8e** and **12b**, but low activity was possessed by compound **15d**, Table 3 and Fig. 4**.**

3.5. Cellular mechanism of action study

3.5.1. Cell cycle inhibition

The most active antitumor compound **8c** was selected for further

Table 3
Percentage inhibition values of target compounds **7a, 7b, 8c, 82, 12b** and **15 d** and lapatinib against EGFR expressed in A549.

Compound ID	EGFR/ A549	
	% inhibition	Conc. ± SEM [a] (ng/ml)
7a	70.05	0.523 ± 7.6
7b	73.32	0.474 ± 14.1
8c	79.25	0.369 ± 13.8
8e	73.01	0.479 ± 9.6
12b	74.41	0.455 ± 8.9
15d	68.39	0.562 ± 3.5
Lapatinib	83.33	0.296 ± 3.06
Control	0	1.777 ± 78.400

(a): IC_{50} values are the mean of seven separate experiments and is a concentration that causes 50% growth inhibition, (b): Standard error of the mean, (c): not tested.

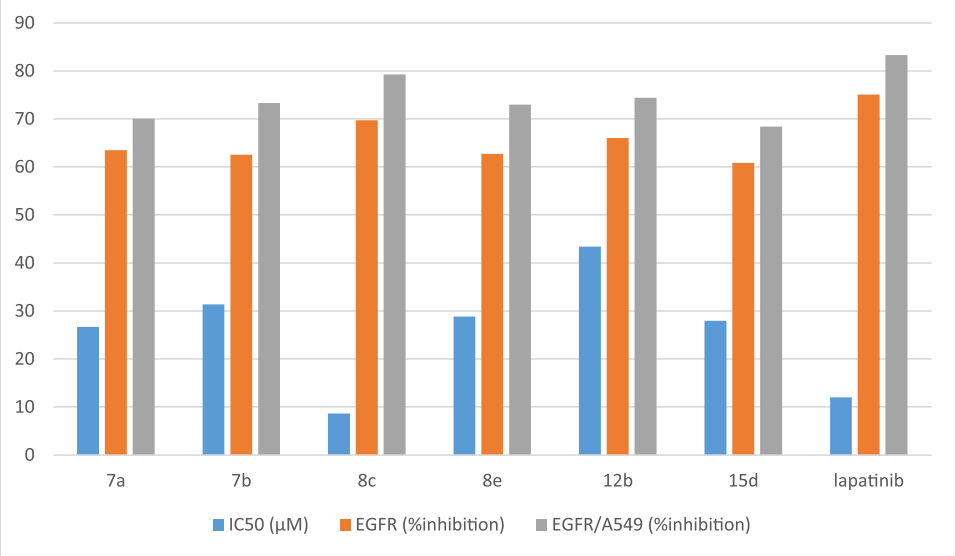

Fig. 4. Cytotoxicity IC_{50}% (μM), cell free EGFR assay (%inhibition) and EGFR (%inhibition) expressed in A549 cells of target compounds **7a, 7b, 8c, 82, 12b** and **15 d** and lapatinib.

study regarding its effect on cell cycle progression and induction of apoptosis in A549 cell line at Vacsera using Propidium Iodide kit and analyzed by Flow Cytometry technique using FACS Calibur reader [38]. The cell line was treated with tested compounds at their IC_{50} values for 24 h. Its effect on the normal cell cycle profile and induction of apoptosis was analyzed. From these results, it was observed that compound **8c** increased concentration at pre G1 (apoptosis) phase (23.87%), if compared to control (1.69%). A significant increase in the percentage at G2/M phase was observed after treatment of cell line with tested compound, indicating that A549 cell line arrested at G2/M phase of cell cycle and contributed to cell cytotoxicity owing to the effect of the tested compound **8c**. On other hand, cell population at G0/G1 and S phase was decreased after treatment with the same compound, if compared to control, Table 4**.**

3.5.2. Cell apoptosis assay

The consequent aptitude of compound **8c** for apoptosis induction was further measured using annexin-V-FITC assay [39]. It was observed that some treated cells were in a late apoptotic stage (upper right quadrant) after a 24 h of treatment of A549 cells (at their IC_{50} concentration) with compound **8c,** Fig. 5. This was indicated by the significant increase in the percentage of annexin V positive and PI positive cells. Compound **8c** showed an increase of 76 folds more than control in late apoptosis. Also, an increase in late apoptosis was noticed over the early one (lower right quadrant), making recovery of apoptotic cells to be healthy more difficult. In conclusion, the tested compound **8c** was able to induce late apoptosis with necrosis percentage = 2.36%, Table 5.

3.5.3. Active Caspase-3 expression level assay

Induction of apoptosis of the tested compound **8c** was further confirmed through assessing caspase-3 expression levels in A549 cell after 24 h treatment using Invitrogen Caspase-3 (active) Human ELISA kit [40]. CASP-3 protein activation plays a key role in the execution-phase of cell apoptosis, Table 6. Caspase-3 activity (in fold change, FLD) significantly increased after cell treatment with compound **8c** (7.94 folds) if compared to control. As expected, the tested compound activated caspase-3 as a mechanism of apoptosis induction, indicating that it not only inhibited proliferation of cancer cells via EGFR inhibition, but also promoted caspase-3 activation and subsequent efficient cell death.

3.6. ADMET studies

Computational studies for predicted pharmacokinetic properties and toxicity of the target compounds **7a, 7b, 8c, 8e, 12b** and **15d** have been performed and results were presented in Table 7**.** ADMET studies were predicted using pkCSM tool (http://biosig.unimelb.edu.au/pkcsm/prediction) [41]. The SMILE molecular structures of the compounds were obtained from PubChem (https://pubchem.ncbi.nlm.nih.gov). The prediction was carried out as a methodological virtual screening, based on various criteria, where all the compounds showed excellent human intestinal absorption results ranging from 86 to 99% absorption. Moreover, human colon adenocarcinoma-2 parameter (Caco2; high Caco2 permeability would translate in values >0.9) showed good results (1.276, 1.286 and 1.436 for compounds **7a, 7b** and **12b**, respectively, thus predicting considerable absorption for orally administered dosage forms of the respective compounds [42], Table 7**.** The volume of distribution calculated using a steady-state volume of distribution (VDss) showed that compounds **8e**, **12b** and **15d** had lower theoretical dose required for uniform distribution in the plasma than compounds **7a**, **7b** and **8c,** while the degree of diffusing across plasma membrane increased in this order; **12b** < **15d** < **7b** < **7a** < **8c** < **8e**, measured as the fraction that is in the unbound state.

On the other hand, BBB permeability of all the compounds was considered promising as the log BB values were below 0.3, thus can be safely used with minimal side effects on the brain, Table 7**.** Furthermore, a group of enzymes that play significant roles in drug metabolism is the CYP isozymes. The tested compounds showed variable range of CYP interactions**,** Table 7. Moreover, predicted *in-silico* toxicity was assessed, where no mutagenic potential of all the tested compounds was observed through AMES toxicity testing. Generally, all the compounds were recorded to act as effective hERG II inhibitors, but not hERG I, the fact that might correlate to subsequent therapeutic cardiac effects [42]. All the compounds showed acceptable safety towards skin sensitization with a liability towards hepatotoxicity induction, Table 7**.**

Collectively, the predicted pharmacokinetic properties and toxicity of the target compounds results confirmed that those newly synthesized compounds did not only show good preferential EGFR inhibitory activities, but also possessed a variable range of promising pharmacokinetic properties that could be used as a versatile tool for future development of promising safely used anticancer agents.

Table 4
Cell cycle analysis of tested compounds in A549 cell line.

Compound ID	Results				
	DNA content %				
	% G0-G1	%S	% G2-M	%Pre G1 (% apoptosis)	Comment
8c/ A549	38.15	26.59	35.26	23.87	cell cycle arrest at G2/M
Control/ A549	57.83	34.28	7.89	1.69	–

3.7. Molecular docking study

Molecular docking study was performed in an attempt to explain the kinase activity of the most active compounds through illustrating their positing and fitting into EGFR active binding site using 'Molecular Operating Environment 2019.0101' software. Moreover, the crystal structure of the enzyme with the reference drug (lapatinib) was obtained from the protein data bank; PDB code: 1XKK [43]. Docking of lapatinib showed the binding mode of lead compound through interaction with two amino acids: Leu718 and Met793 through pi-bonds and hydrogen bond acceptor, respectively, into the active site of EGFR enzyme, Fig. 6**.** In the present study, it was found that compound **8c** was bound to EGFR enzyme active site (Energy affinity −13.19 kcal/mol) in a similar mode as that of the reference drug, lapatinib, through hydrogen bond acceptor to Leu792 and key amino acid Met793 via sulphonyl oxygen, respectively, in addition to an extra pi-bond with Met793 via phenyl ring of sulphonamide moiety (**Supplementary tables, S3**). Its proper interaction explained its potency as EGFR inhibitor. However, a moderate EGFR inhibitory activity for compounds **7a,b** and **8e** and which was contributed to their retention of pi-bond interaction of phenyl ring of quinazoline nucleus with key amino acid Leu718. However, their interaction with different amino acids for each compound was clear except for compound **12b**, which did not interact with the main amino acid, but instead it showed seven binding interactions with five different amino acids. Also, binding interactions of compound **15d** with key amino acids (Leu718 or Met793) were not visible, the fact that coincided with preceding *in vitro* biological results. On the other hand, compounds **12b** and **15d** showed two binding interaction via H-donor and H-acceptor binding with Asp855 in addition to Arg841 interaction with pi-bond (**Supplementary figures, S1**). The overall docking results of the tested compounds came out to confirm all the above mentioned biological *in vitro* EGFR inhibitory activities. Collectively, compound **8c** showed potent EGFR inhibition activity similar to that of lapatinib, where other tested compounds possessed moderate to weak activities. The activity of compound **8c** could be attributed to good binding affinity of sulphonyl oxygen via H-bond acceptor to Leu792 and Met793, the key amino acids of EGFR enzyme, in addition to an extra pi-bond between the phenyl ring of sulphonamide moiety and Met793 amino acid. Also,

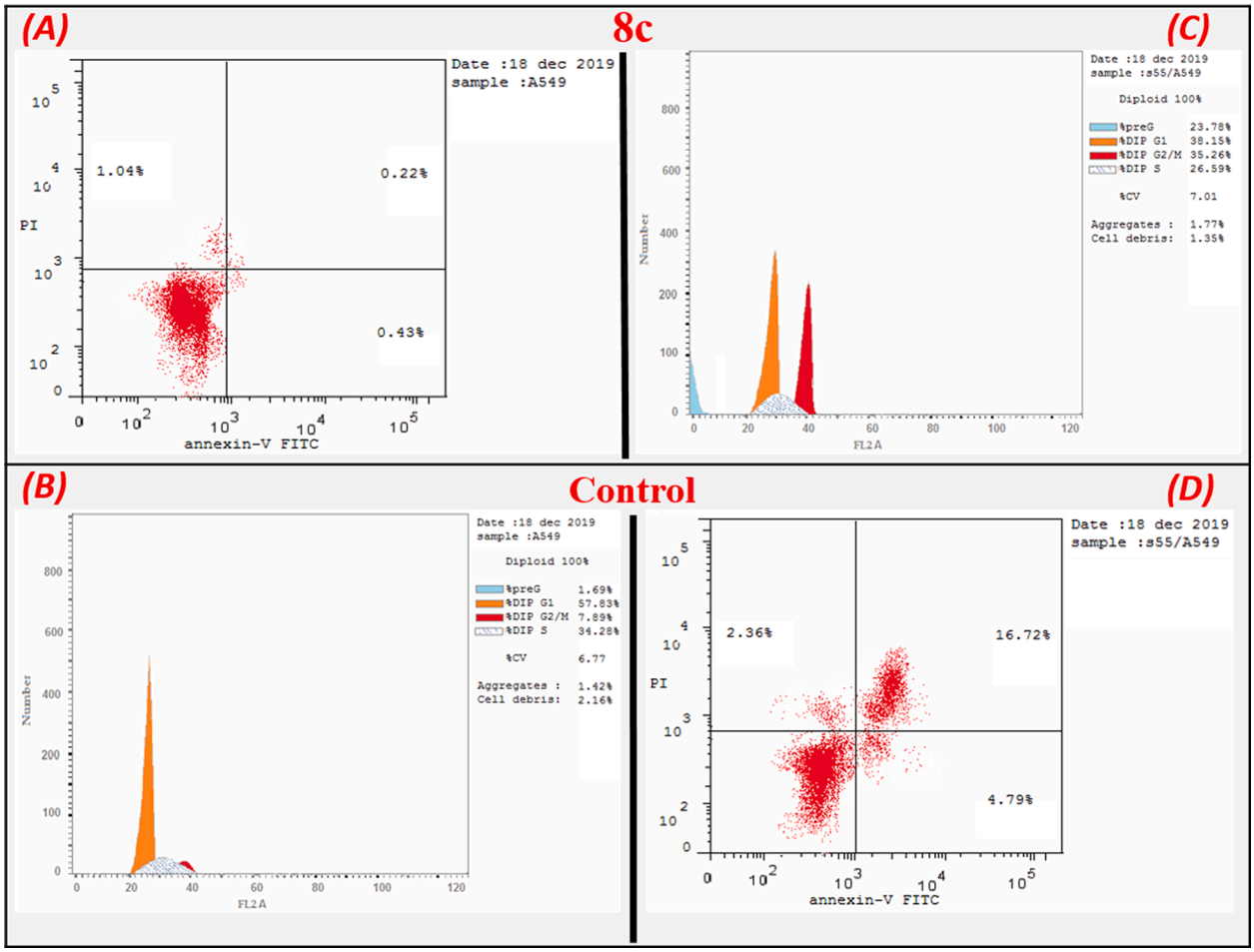

Fig. 5. Effect of compound **8c** *(A)* and control *(B)* on DNA-ploidy flow cytometric analysis of A549. Representative dot plots of A549 cells treated with compound **8c** *(C)* and control *(D)* for 24 h and analyzed by flow cytometry after double staining of the cells with Annexin-V FITC and PI.

Table 5
Effect of tested compounds on apoptosis and necrosis in A549.

Compound. ID	Apoptosis			Necrosis
	Total	Early	Late	
8c/A549	23.87	4.79	16.72	2.36
Control. A549	1.69	0.43	0.22	1.04

Table 6
Effect of tested compounds on Caspase-3 expression level in A549.

Compound ID	Results	
	Casp3/ A549	
	Conc (pg/ml)	FLD
8c	319.9 ± 9.55	7.94
Control	40.28 ± 6.2	1

the methoxystyryl moiety, which has been embedded in hydrophobic region of EGFR enzyme, has significantly contributed to the considerable anticancer efficacy of compound **8c** through implied EGFR inhibition.

4. Conclusion

Wrapping up the present research work and results, it could be briefly stated that novel quinazoline hybrids (**7a-e**, **8a-e**, **12a-e** and **15a-d)** have been designed and synthesized. Those hybrids firstly started with synthesizing two new series of 2,4-disubstituted quinazoline derivatives **7a-e** and **8a-e** through fixing a *p*-methoxystyryl moiety at position 2 of the quinazoline backbone, then followed by the incorporation of either substituted anilino derivatives or sulfonamide derivatives, respectively, at position 4 of the quniazoline core. Further experimental chemistry work was conducted on two most potent representatives from each series; **7b** (4- *p*-chlorophenylanilino) and **8c** (4-oxazolylbenzenesulfonamide) to result in another two new quinazoline series **12a-e** and **15a-d,** respectively. All the compounds of the four series were evaluated for their *in vitro* anticancer activities (nine subpanels) at the National Cancer Institute (NCI), USA. Accordingly, it was concluded that compound **8c**, a quinazoline backbone hybridized with a methoxystyryl moiety at position 2 and an isoxazolylbenzenzensulfonamide moiety at position 4, exhibited the best pharmacological results. It showed broad spectrum anti-cancer activity with potent efficacy against A549 cell line (IC_{50} = 8.62 μM), almost double that of lapatinib (IC_{50} = 11.98 μM), while compounds **7a,b, 8e** and **12b** revealed moderate activities. Further mechanistic biological investigation was conducted through cytotoxicity studies against NSLC (A549), non-cell EGFR, EGFR expressed in A549 cell line assays, in addition to molecular modeling studies. The research observation has recorded that generally substitution of the quinazoline nucleus at position 2 with *p*-methoxystyryl moiety derivative resulted in potent broad spectrum anti-tumor activity that was enhanced by an oxazolyl benzensulfonamide moiety at position 4 as in compound **8c**. Otherwise, replacement of *p*-methoxystyryl moiety at position 2 or other substituted anilino derivatives at position 4 led to moderate or low activities. The observed good activity of compound **8c**

Table 7
Predicted pharmacokinetic properties and toxicity of the target compounds **7a, 7b, 8c, 8e, 12b** and **15d.**

Model Name (Unit)	Predicted Value					
	7a	**7b**	**8c**	**8e**	**12b**	**15d**
Lipophilicity (LogP)	5.561	6.206	5.649	5.452	5.903	5.052
Intestinal absorption- human (%)	93.759	92.093	99.694	96.647	90.926	86.744
Caco2 permeability (log Papp in 10–6 cm/s)	1.276	1.286	−0.248	−0.065	1.436	−0.096
VDss- human (log L/kg)	−0.635	−0.532	−0.756	−0.839	−0.937	−1.032
Fraction unbound- human	0.164	0.157	0.169	0.182	0.029	0.044
BBB permeability (log BB)	0.020	0.108	−1.441	−1.494	0.052	−1.936
CYP2D6 substrate/ inhibitor	No	No	No	No	No	No
CYP3A4 substrate/ inhibitor	Yes	Yes	Yes	Yes	Yes	Yes
AMES toxicity (Categorical: Yes/No)	No	No	No	No	No	No
hERG I inhibitor (Categorical: Yes/No)	No	No	No	No	No	No
hERG II inhibitor (Categorical: Yes/No)	Yes	Yes	Yes	Yes	Yes	Yes
Hepatotoxicity (Categorical: Yes/No)	Yes	Yes	Yes	Yes	Yes	Yes
Skin Sensitisation (Categorical: Yes/No)	No	No	No	No	No	No

Caco2: Human colon adenocarcinoma-2, VDss: Steady-state volume of distribution, BBB: Blood-brain barrier, AMES: Salmonella typhimurium reverse mutation assay, hERG: Human ether-a-go-go-related gene.

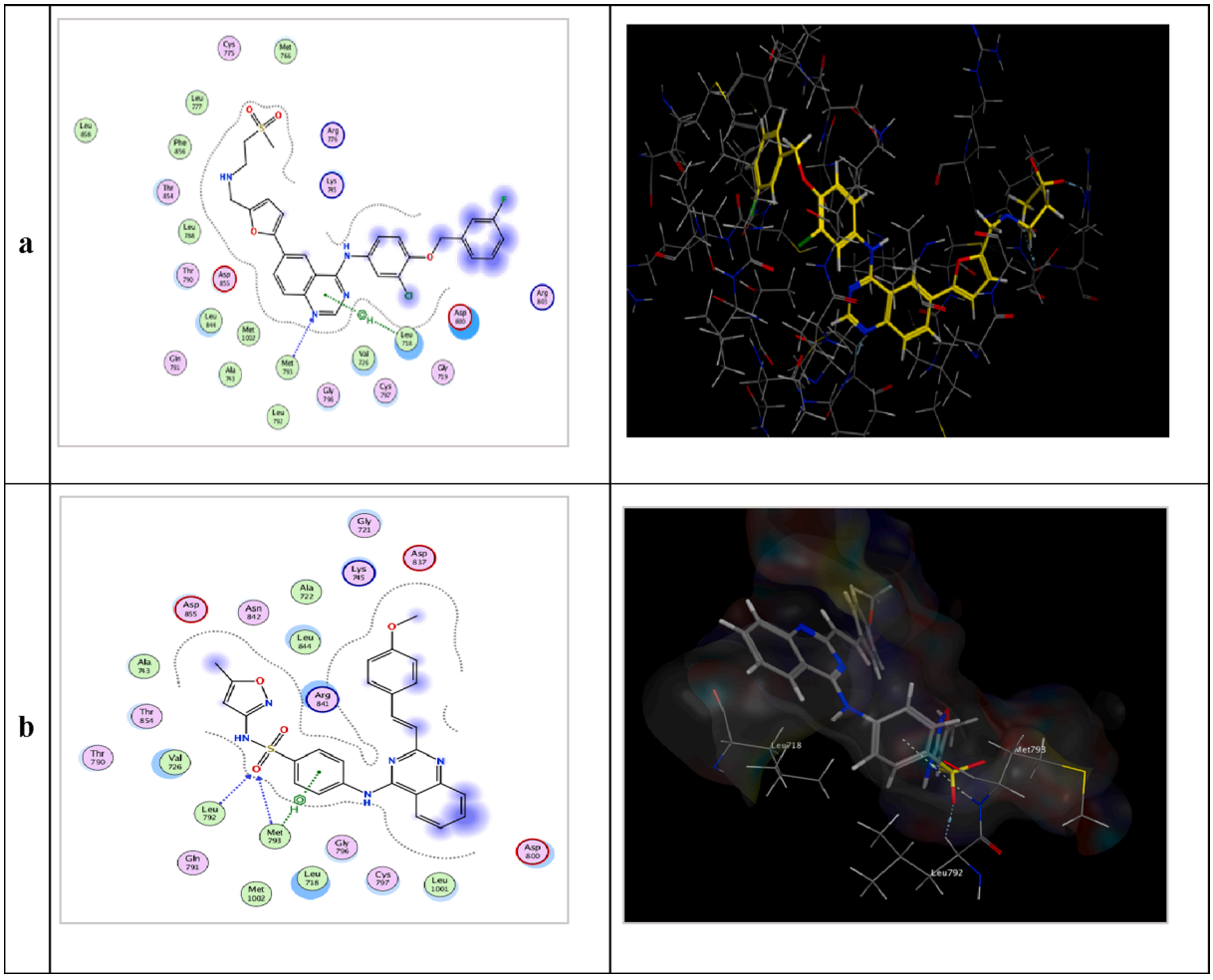

Fig. 6. 2D and 3D Docking of (a) lapatinib and (b) compound **8c** into active binding site of EGFR (using PDB code: 1XKK).

has been attributed to good binding affinity of the sulphonyl oxygen via H-bond acceptor to Leu792 and Met793, the key amino acids of EGFR enzyme, in addition to an extra Pi-bond between phenyl ring of sulphonamide moiety and Met793 amino acid, not to mention the effect of the methoxystyryl moiety through its pretty inclusion within the hydrophobic region of EGFR enzyme. Collectively, it could be safely concluded that compound **8c** possessed a good apoptosis induction activity in addition to considerable EGFR inhibitory activity. Moreover, it was hypothesized that further derivatization of the most active compound **8c** in the upcoming future could result in promising potent antitumor activity with improved EGFR selectivity and thus higher safety profiles.

5. Experimental

5.1. Chemistry

Melting points were carried out by open capillary tube method using IA 9100 MK-Digital Melting Point Griffin Apparatus and were uncorrected. Elemental Microanalyses were carried out using Vario El III, CHNSO analyzer (Germany) at Faculty of Pharmacy, Al-azhar University. Infrared Spectra were done on Bruker FT-IR spectrophotometer Vector 22, Schimadzu 435, Perkin-Elmer 457 and Jasco FT.IR plus 460 Japan and expressed in wave number (cm^{-1}), using KBr discs. ^{1}H NMR Spectra were carried out using Bruker Avance III at 400 MHz (Bruker AG, Switzerland) using DMSO-d_6 or otherwise stated as a solvent. The chemical shifts were expressed in δ ppm units using trimethylsilane as the internal standard. ^{13}C NMR spectra were carried out using Bruker Avance III at 100 MHz (Bruker AG, Switzerland) using DMSO-d_6 as a solvent. Mass Spectra was done on Shimadzu Qp- 2010 plus. All the reactions were monitored by thin layer chromatography. Silica gel/TLC-cards DC- Alufolien-Kieselgel with fluorescent indicator 254 nm; layer thickness 0.2 mm. Petroleum ether: ethyl acetate (1:1) or (1:2) was the adopted solvent system.

5.1.1. Materials

Compounds **3** [30], **5**,**6** [31] and **9** [32] were synthesized acorrding to the reported procedures.

5.1.2. General procedure for the synthesis of compounds (7a-e)

The appropriate amino derivative (10 mmole) was added to a solution of (E)-4-chloro-2-(4-methoxystyryl) quinazoline **6** (1.23 g, 10 mmole) in dry DMF (15 mL) in presence of potassium carbonate (1.23 g, 10 mmole), except for compounds **7a** and **7c** that were stirred in isopropanol and ethylene glycol, respectively. The reaction mixture was then refluxed for 24 h and poured onto ice/water, then the solution was acidified with acetic acid (pH 7). The resulting precipitate was filtered, washed with water, dried and re-crystallized from aqueous ethanol.

*5.1.2.1. (E)-4-((2-(4-Methoxystyryl)quinazolin-4-yl)amino)phenol **(7a)**.* Yield 64%; mp 202–204 °C. IR (ν_{max}/cm^{-1}): 3363, 3248 (OH, NH), 3132, 2924 (CH aromatic, CH aliphatic). ^{1}H NMR δ ppm: 3.63 (s, 3H, OCH_3), 5.92 (s, 1H, OH, exch. D_2O), 6.59 (d, 2H, CH aromatic, J = 8.4 Hz), 6.66 (d, 1H, CH═CH, J = 14.4 Hz), 6.78 (d, 2H, CH aromatic, J = 8.4 Hz), 7.02 (d, 2H, CH aromatic, J = 8.8 Hz), 7.16 (d, 2H, CH aromatic, J = 8.8 Hz), 7.42 (t, 1H, CH aromatic, J = 9.8 Hz), 7.56 (d, 1H, CH aromatic, J = 8.0 Hz), 7.74 (t, 1H, CH aromatic, J = 15.34 Hz), 8.06 (d, 1H, CH aromatic, J = 7.8 Hz), 9.46 (s, 1H, NH, exch. D_2O). ^{13}C NMR δ ppm: 55.86 (OCH_3), 115.35, 115.95, 116.25, 121.09, 124.69, 124.88, 126.14, 126.31, 127.04, 130.58, 142.58, 149.43, 152.89, 154.58, 155.65, 162.22 (aromatic Cs), 123.34, 134.73 (2 olefinic Cs). Mass (m/z): 369 (M^+, 9.74), 159 (100). Anal. Calcd for $C_{23}H_{19}N_3O_2$ (369.42): C, 74.78; H, 5.18; N, 11.37. Found: C, 75.01; H, 5.34; N, 11.63%.

*5.1.2.2. (E)-N-(4-Chlorophenyl)-2-(4-methoxystyryl)quinazolin-4-amine **(7b)**.* Yield 65%; mp 226–228 °C. IR (ν_{max}/cm^{-1}): 3263 (NH), 3186, 2927 (CH aromatic, CH aliphatic). ^{1}H NMR δ ppm: 3.82 (s, 3H, OCH_3), 6.79 (d, 1H, CH═CH, J = 16.4 Hz), 6.96 (d, 2H, CH aromatic, J = 8.4 Hz), 7.49 (d, 2H, CH aromatic, J = 8.8 Hz), 7.55 (t, 1H, CH aromatic, J = 15.6 Hz), 7.61 (d, 2H, CH aromatic, J = 7.6 Hz), 7.75 (d, 1H, CH aromatic, J = 8.0 Hz), 7.79–7.86 (m, 2H, CH aromatic, CH═CH), 7.97 (d, 2H, CH aromatic, J = 8.0 Hz), 8.06 (d, 1H, CH aromatic, J = 7.6 Hz), 9.85 (s, 1H, NH, exch. D_2O). ^{13}C NMR δ ppm: 55.71 (OCH_3), 114.81, 115.01, 121.48, 123.58, 126.11, 126.91, 127.35, 128.16, 128.82, 129.72, 134.75, 138.99, 151.04, 157.55, 160.38, 161.05 (aromatic Cs), 123.53, 133.62 (2 olefinic Cs). Mass (m/z): 387 (M^+, 86.3), 386 (100). Anal. Calcd for $C_{23}H_{18}ClN_3O$ (387.86): C, 71.22; H, 4.68; N, 10.83. Found: C, 70.89; H, 4.84; N, 11.15%.

*5.1.2.3. (E)-2-(4-Methoxystyryl)-N-(4-nitrophenyl)quinazolin-4-amine **(7c)**.* Yield 57%; mp 241–243 °C. IR (ν_{max}/cm^{-1}): 3448 (NH) 3119, 2924 (CH aromatic, CH aliphatic). ^{1}H NMR δ ppm: 3.80 (s, 3H, OCH_3), 6.60 (d, 2H, CH aromatic, J = 9.2 Hz), 6.89 (d, 1H, CH═CH, J = 16.0 Hz), 7.00 (d, 2H, CH aromatic, J = 8.8 Hz), 7.11 (d, 2H, CH aromatic, J = 8.8 Hz), 7.62 (t, 1H, CH aromatic, J = 10.4 Hz), 7.86 (d, 1H, CH aromatic, J = 7.6 Hz), 7.92 (t, 1H, CH aromatic, J = 9.8 Hz), 8.08 (d, 1H, CH aromatic, J = 7.6 Hz), 8.18 (d, 1H, CH═CH, J = 8.4 Hz), 8.25 (d, 2H, CH aromatic, J = 8.8 Hz), 9.85 (s, 1H, NH, exch. D_2O). ^{13}C NMR δ ppm: 55.78 (OCH_3), 112.84, 115.00, 121.51, 122.37, 126.31, 126.86, 127.20, 128.21, 128.94, 129.71, 134.63, 138.07, 152.06, 157.16, 160.96, 162.07 (aromatic Cs), 123.05, 134.18 (2 olefinic Cs). Mass (m/z): 398 (M^+, 11.77), 277 (100). Anal. Calcd for $C_{23}H_{18}N_4O_3$ (398.41): C, 69.34; H, 4.55; N, 14.06. Found: C, 69.01; H, 4.79; N, 14.32%.

*5.1.2.4. (E)-Ethyl 4-((2-(4-methoxystyryl)quinazolin-4-yl)amino)benzoate **(7d)**.* Yield 62%; mp 267–269 °C. IR (ν_{max}/cm^{-1}): 3441 (NH), 3150, 2920 (CH aromatic, CH aliphatic), 1666 (CO). ^{1}H NMR δ ppm: 1.25 (t, 3H, CH_3, J = 10.6 Hz), 3.86 (s, 3H, OCH3), 4.17 (q, 2H, CH_2, J = 8.0 Hz), 6.55 (d, 1H, CH═CH, J = 8.4 Hz), 7.02 (d, 2H, CH aromatic, J = 8.8 Hz), 7.11 (d, 2H, CH aromatic, J = 8.4 Hz), 7.46 (t, 1H, CH aromatic, J = 10.12 Hz), 7.60–7.65 (m, 4H, CH aromatic), 7.72 (d, 1H, CH aromatic, J = 8.4 Hz), 7.86 (t, 1H, CH aromatic, J = 10.0 Hz), 8.09 (d, 1H, CH═CH, J = 8.4 Hz), 8.20 (d, 1H, CH aromatic, J = 7.6 Hz), 12.21 (s, 1H, NH, exch. D_2O). ^{13}C NMR δ ppm: 14.66 (CH3), 55.79 (OCH3), 78.57 (CH2), 113.08, 114.38, 115.02, 115.45, 119.18, 121.44, 126.32, 127.37, 128.14, 128.92, 129.75, 130.46, 138.41, 149.62, 152.52, 161.07 (aromatic carbons), 121.11, 134.85 (2 olefinic Cs), 162.64 (C═O). Mass (m/z): 425 (M^+, 1.06), 70 (100). Anal. Calcd for $C_{25}H_{21}N_3O_3$ (425.17): C, 72.98; H, 5.14; N, 10.21. Found: C, 72.69; H, 5.82; N, 10.44%.

*5.1.2.5. (E)-N-(4-((2-(4-Methoxystyryl)quinazolin-4-yl)amino)phenyl) acetamide **(7e)**.* Yield 60%; mp 250–252 °C IR (ν_{max}/cm^{-1}): 3444, 3280 (NHs), 3120, 2924 (CH aromatic, CH aliphatic), 1674 (CO). ^{1}H NMR δ ppm: 2.00 (s, 3H, CH_3), 3.82 (s, 3H, OCH_3), 6.65 (d, 2H, CH aromatic, J = 8.0 Hz), 6.86 (d, 1H, CH═CH, J = 16.0 Hz), 6.91 (d, 2H, CH aromatic, J = 8.0 Hz), 7.03 (d, 2H, CH aromatic, J = 8.0 Hz), 7.44 (t, 1H, CH aromatic, J = 16.0 Hz), 7.62–7.67 (m, 3H, CH aromatic), 7.78 (t, 1H, CH aromatic, J = 16.0 Hz), 7.90 (d, 1H, CH═CH, J = 16.0 Hz), 8.10 (d, 1H, CH aromatic, J = 8.0 Hz), 9.62 (s, 1H, NH, exch. D_2O). ^{13}C NMR δ ppm: 24.51 (CH_3), 55.80 (OCH_3), 114.76, 115.04, 119.00, 121.42, 123.93, 126.32, 127.50, 128.09, 129.28, 129.77, 137.39, 139.29, 152.34, 157.89, 161.11, 162.83 (aromatic Cs), 122.52, 134.93 (2 olefinic Cs), 168.20 (C═O). Mass (m/z): 395 (M^+, 9.07), 54 (100). Anal. Calcd for $C_{25}H_{21}N_3O_2$ (395.45): C, 75.93; H, 5.35; N, 10.63. Found: C, 75.69; H, 5.57; N, 10.86%.

5.1.3. General procedure for the synthesis of compounds (8a-e)

A mixture of 4-chloro-2-(4-methoxystyryl)quinazoline **(6)** (0.89 g, 10 mmole) and appropriate sulphonamide derivative (10 mmole) was refluxed in ethanol (10 mL) in presence of anhydrous potassium carbonate (1.38 g, 10 mmole) for 24 h. The reaction mixture was then cooled, poured onto ice/water and acidified with acetic acid (pH 6). The resulting precipitate was filtered, washed with water, dried and re-crystallized from aqueous ethanol.

*5.1.3.1. (E)-N-((4-((2-(4-Methoxystyryl)quinazolin-4-yl)amino)phenyl) sulfonyl)acetamide **(8a)**.* Yield 72%; mp 238–240 °C. IR (ν_{max}/cm^{-1}): 3368, 3186 (NHs), 3132, 2954 (CH aromatic, CH aliphatic), 1674 (CO), 1300, 1149 (SO_2).^{1}H NMR δ ppm: 2.09 (s, 3H, CH_3), 3.81 (s, 3H, OCH_3), 6.86 (d, 1H, CH═CH, J = 16.0 Hz), 7.01 (d, 2H, CH aromatic, J = 8.8 Hz), 7.43 (t, 1H, CH aromatic, J = 14.8 Hz), 7.61–6.66 (m, 5H, CH aromatic), 7.75 (d, 2H, CH aromatic, J = 8.4 Hz), 7.78 (t, 1H, CH aromatic, J = 14.4 Hz), 7.88 (d, 1H, CH═CH, J = 16.00 Hz), 8.09 (d, 1H, CH aromatic, J = 7.6 Hz), 10.40 (s, 1H, NH, exch. D_2O). ^{13}C NMR δ ppm:

24.57 (CH_3), 55.78 (OCH_3), 115.02, 118.89, 119.08, 121.44, 126.14, 126.32, 127.13, 127.36, 128.11, 129.75, 134.45, 138.46, 149.59, 152.41, 161.08, 162.43 (aromatic Cs), 122.50, 134.85 (2 olefinic Cs), 170.02 (C═O). Mass (*m/z*): 475 (M^+, 6.19), 255 (100). Anal. Calcd for $C_{25}H_{22}N_4O_4S$ (474.53): C, 63.28; H, 4.67; N, 11.81. Found: C, 63.06; H, 4.85; N, 12.04%.

5.1.3.2. (E) - N- carbamimidoyl −4-((2- (4-methoxystyryl) quinazolin- 4-yl) amino) benzene sulfonamide ***(8b)***. Yield 68%; mp 260–262 °C. IR (ν_{max}/cm^{-1}): 3402, 3344 (NHs, NH2), 3224, 2954 (CH aromatic, CH aliphatic), 1678 (CO), 1307, 1130 (SO_2).^{1}H NMR δ ppm: 3.79 (s, 3H, OCH_3), 5.70 (s, 1H, NH, exch. D_2O), 6.56 (d, 2H, CH aromatic, $J = 4.2$ Hz), 6.93 (d, 1H, CH═CH, $J = 16.0$ Hz), 6.98 (d, 2H, CH aromatic, $J = 8.4$ Hz), 7.41(d, 2H, CH aromatic, $J = 8.4$ Hz), 7.61 (d, 2H, CH aromatic, $J = 8.8$ Hz), 7.70 (t, 1H, CH aromatic, $J = 16.0$ Hz), 7.78 (d, 1H, CH aromatic, $J = 8.0$ Hz), 7.86 (t, 1H, CH aromatic, $J = 16.0$ Hz), 7.95 (d, 1H, CH═CH, $J = 16.0$ Hz), 8.08 (d, 1H, CH aromatic, $J = 8.4$ Hz), 8.53 (s, 1H, NH_2, exch. D_2O), 9.86 (s, 1H, NH, exch. D_2O). ^{13}C NMR δ ppm: 55.75 (OCH_3), 112.82, 114.81, 114.93, 121.37, 126.28, 127.29, 127.70, 129.55, 129.70, 131.27, 132.30, 134.48, 137.95, 151.79, 158.53, 160.75 (aromatic Cs), 121.57, 133.94 (2 olefinic Cs), 175.57 (C = NH). Mass (*m/z*): 475 (M^+, 10.40), 81 (100). Anal. Calcd for $C_{24}H_{22}N_6O_3S$ (474.53): C, 60.75; H, 4.67; N, 17.71. Found: C, 60.54; H, 4.80; N, 17.53%.

5.1.3.3. (E)- 4- ((2- (4- Methoxystyryl) quinazolin- 4- yl) amino)- N- (5-methylisoxazol- 3- yl) benzenesulfonamide ***(8c)***. Yield 70%; mp 272–274 °C. IR (ν_{max}/cm^{-1}): 3471, 3387 (NHs), 3186, 2927(CH aromatic, CH aliphatic), 1465, 1172 (SO_2).^{1}H NMR δ ppm: 2.31 (s, 3H, CH_3), 3.83 (s, 3H, OCH_3), 6.22 (s, 1H, CH isoxazole), 6.85 (d, 1H, CH═CH, $J = 16.0$ Hz), 7.03 (d, 2H, CH aromatic, $J = 8.8$ Hz), 7.14 (d, 2H, CH aromatic, $J = 8.0$ Hz), 7.46 (t, 1H, CH aromatic, $J = 14.4$ Hz), 7.62 (d, 2H, CH aromatic, $J = 8.8$ Hz), 7.66 (d, 2H, CH aromatic, $J = 8.4$ Hz), 7.72 (d, 1H, CH aromatic, $J = 8.4$ Hz), 7.79 (t, 1H, CH aromatic, $J = 14.8$ Hz), 7.91 (d, 1H, CH═CH, $J = 15.6$ Hz), 8.10 (d, 1H, CH aromatic, $J = 8.00$ Hz), 12.29 (s, 1H, NH, exch. D_2O). ^{13}C NMR δ ppm: 12.70 (CH_3), 55.78 (OCH_3), 99.89, 112.70, 114.86, 115.02, 119.08, 126.32, 127.36, 127.82, 128.11, 129.75, 135.17, 138.25, 138.46, 149.58, 152.42, 161.09, 162.43 (aromatic Cs), 121.44, 134.86 (2 olefinic Cs). Mass (*m/z*): 514 (M^+, 4.22), 67 (100). Anal. Calcd for $C_{27}H_{23}N_5O_4S$ (513.57): C, 63.14; H, 4.51; N, 13.64. Found: C, 63.47; H, 4.78; N, 13.92%.

5.1.3.4. (E) − 4- ((2- (4 -Methoxystyryl) quinazolin- 4-yl) amino)- N-(pyrimidin-2- yl) benzenesulfonamide ***(8d)***. Yield 68%; mp 268–270 °C. IR (ν_{max}/cm^{-1}): 3425, 3356 (NHs), 3105, 2935 (CH aromatic, CH aliphatic), 1442, 1153 (SO_2). ^{1}H NMR δ ppm: 3.80 (s, 3H, OCH_3), 6.02 (d, 2H, CH aromatic, $J = 8.0$ Hz), 6.56 (t, 1H, CH aromatic, $J = 16.0$ Hz), 6.85 (d, 1H, CH═CH, $J = 16.0$ Hz), 7.03 (d, 2H, CH aromatic, $J = 8.0$ Hz), 7.45 (t, 1H, CH aromatic, $J = 16.0$ Hz), 7.62–7.67 (m, 5H, CH aromatic), 7.79 (t, 1H, CH aromatic, $J = 16.0$ Hz), 7.91 (d, 1H, CH═CH, $J = 16.0$ Hz), 8.10 (d, 1H, CH aromatic, $J = 8.0$ Hz), 8.49 (d, 2H, CH aromatic, $J = 4.4$ Hz), 11.29 (s, 1H, NH, exch. D_2O), 12.28 (s, 1H, NH, exch. D_2O). ^{13}C NMR δ ppm: 55.79 (OCH_3), 112.51, 114.10, 114.86, 115.02, 118.97, 126.32, 126.39, 127.35, 127.87, 128.09, 129.79, 129.84, 132.29, 138.54, 149.52, 152.55, 158.34, 159.72, 161.10 (aromatic Cs), 121.41, 134.92 (2 olefinic Cs). Mass (*m/z*): 511 (M^+, 5.14), 69 (100). Anal. Calcd for $C_{27}H_{22}N_6O_3S$ (510.57): C, 63.52; H, 4.34; N, 16.46. Found: C, 63.19; H, 4.47; N, 16.80%.

5.1.3.5. (E)-N- (4, 6- dimethylpyrimidin −2-yl) −4- ((2- (4- methoxystyryl) quinazolin-4- yl) amino) benzenesulfonamide ***(8e)***. Yield 65%; mp 229–231 °C. IR (ν_{max}/cm^{-1}): 3471, 3356 (NHs), 3186, 2931 (CH aromatic, CH aliphatic), 1419, 1172 (SO_2).^{1}H NMR δ ppm: 2.04 (s, 6H, $2CH_3$), 3.84 (s, 3H, OCH_3), 6.80 (s, 1H, CH aromatic), 6.83 (d, 1H, CH═CH, $J = 15.6$ Hz), 6.96 (d, 2H, CH aromatic, $J = 8.8$ Hz), 7.10 (d, 2H, CH aromatic, $J = 8.8$ Hz), 7.43 (t, 1H, CH aromatic, $J = 14.4$ Hz), 7.55–7.62 (m, 4H, CH aromatic), 7.65 (d, 1H, CH aromatic, $J = 8.0$ Hz), 7.70 (t, 1H, CH aromatic, $J = 17.6$ Hz), 7.88 (d, 1H, CH═CH, $J = 12.4$ Hz), 8.11 (d, 1H, CH aromatic, $J = 7.6$ Hz), 9.86, 10.31 (s, 2H, NH, exch. D_2O). ^{13}C NMR δ ppm: 24.54 ($2CH_3$), 55.74 (OCH_3), 114.90, 115.03, 118.30, 118.94, 124.33, 126.32, 127.39, 128.08, 128.73, 129.57, 129.77, 132.28, 138.54, 149.55, 152.26, 160.68, 161.11, 162.31, 172.56 (aromatic Cs), 121.42, 134.92 (2 olefinic Cs). Mass (*m/z*): 539 (M^+, 34.16), 55 (100). Anal. Calcd for $C_{29}H_{26}N_6O_3S$ (538.62): C, 64.76; H, 4.87; N, 15.60. Found: C, 64.52; H, 5.12; N, 15.89%.

5.1.4. Synthesis of N-(4-Chlorophenyl)-2-methylquinazolin-4-amine ***(11)***

Para-chloroaniline (1.23 g, 10 mmole) was added to a solution of 4-chloro-2-methylquinazoline **9** (1.23 g, 10 mmole) in DMF (15 mL) in presence of potassium carbonate (1.23 g, 10 mmole). The reaction mixture was refluxed for 24 h and poured onto ice/water, then the solution was acidified with acetic acid (pH 7). The resulting precipitate was filtered, washed with water, dried and recrystallized from aqueous ethanol. Yield 70%; mp 270–272 °C. IR (ν_{max}/cm^{-1}): 3398 (NH), 3186, 2931 (CH aromatic, aliphatic). ^{1}H NMR δ ppm: 2.35 (s, 3H, CH_3), 7.37 (d, 2H, CH aromatic, $J = 8.8$ Hz), 7.42 (t, 1H, CH aromatic, $J = 14.8$ Hz), 7.55 (d, 1H, CH aromatic, $J = 8.4$ Hz), 7.62 (d, 2H, CH aromatic, $J = 8.8$ Hz), 7.74 (t, 1H, CH aromatic, $J = 15.2$ Hz), 8.06 (d, 1H, CH aromatic, $J = 7.6$ Hz), 8.55 (s, 1H, NH, exch. D_2O). Mass (*m/z*): 270 (M+, 45), 167 (100). Anal. Calcd for $C_{15}H_{12}ClN_3$ (269.73): C, 66.79; H, 4.48; N, 15.58. Found: C, 66.51; H, 4.67; N, 15.84%.

5.1.5. General procedure for the synthesis of compounds ***(12a-e)***

The appropriate aldehyde (20 mmole) was added to a solution of N-(4-chlorophenyl)-2-methylquinazolin-4-amine **11** (2.7 g, 10 mmole) in glacial acetic acid (10 mL) in presence of sodium acetate (1.6 g, 20 mmole) and refluxed for 24 h. The product was poured onto ice/water, filtered off, dried and crystallized from ethanol to give the desired compound.

5.1.5.1. (E)-4-(2-(4-((4-Chlorophenyl)amino)quinazolin-2-yl)vinyl) phenol ***(12a)***. Yield 64%; mp 388–390 °C. IR (ν_{max}/cm^{-1}): 3417, 3341 (NH, OH), 3126, 2924 (CH aromatic, CH aliphatic). ^{1}H NMR δ ppm: 6.37 (d, 2H, CH aromatic, $J = 8.4$ Hz), 6.72 (d, 2H, CH aromatic, $J = 8.0$ Hz), 6.95 (d, 1H, CH═CH, $J = 15.6$ Hz), 7.07 (d, 2H, CH aromatic, $J = 8.4$ Hz), 7.40–7.44 (m, 3H, CH aromatic), 7.54 (d, 1H, CH aromatic, $J = 7.6$ Hz), 7.72 (t, 1H, CH aromatic, $J = 16.0$ Hz), 7.90 (d, 1H, CH═CH, $J = 16.0$ Hz), 8.05 (d, 1H, CH aromatic, $J = 7.6$ Hz), 8.52 (s, 1H, NH, exch. D_2O), 9.40 (s, 1H, OH, exch. D_2O). ^{13}C NMR δ ppm: 115.50, 119.02, 121.83, 125.96, 126.15, 126.76, 129.76, 131.04, 132.92, 149.60, 163.22, 167.06, 175.57, 188.23 (aromatic Cs), 121.05, 134.42 (2 olefinic Cs). Mass (*m/z*): 374 (M^+, 18.9), 124 (100). Anal. Calcd for $C_{22}H_{16}ClN_3O$ (373.83): C, 70.68; H, 4.31; N, 11.24. Found: C, 70.94; H, 4.47; N, 11.56%.

5.1.5.2. (E)-N-(4-Chlorophenyl)-2-(4-chlorostyryl)quinazolin-4-amine ***(12b)***. Yield 65%; mp 301–303 °C. IR (ν_{max}/cm^{-1}): 3309 (NH), 3186, 2931 (CH aromatic, CH aliphatic). ^{1}H NMR δ ppm: 7.00 (d, 1H, CH═CH, $J = 16.4$ Hz), 7.17 (d, 2H, CH aromatic, $J = 8.2$ Hz), 7.24 (d, 2H, CH aromatic, $J = 8.0$ Hz), 7.47–7.53 (m, 3H, CH aromatic), 7.68–7.70 (m, 3H, CH aromatic), 7.81 (t, 1H, CH aromatic, $J = 15.2$ Hz), 7.91 (d, 1H, CH═CH, $J = 16.0$ Hz), 8.11 (d, 1H, CH aromatic, $J = 7.6$ Hz), 12.33 (s, 1H, NH, exch. D_2O). ^{13}C NMR δ ppm: 115.90, 122.32, 126.35, 126.83, 127.59, 129.58, 129.78, 130.34, 134.68, 135.04, 137.35, 151.72, 156.26, 162.23 (aromatic Cs), 121.57, 134.39 (2 olefinic Cs). Mass (*m/z*): 392 (M^+, 12.5), 75 (100). Anal. Calcd for $C_{22}H_{15}Cl_2N_3$ (392.28): C, 67.36; H, 3.85; N, 10.71. Found: C, 67.04; H, 4.12; N, 11.04%.

*5.1.5.3. (E)-N-(4-Chlorophenyl)-2-(4-nitrostyryl)quinazolin-4-amine **(12c)**.* Yield 60%; mp 356–358 °C. IR (νmax/cm-1): 3305 (NH), 3124, 2927 (CH aromatic, CH aliphatic). ^{1}H NMR δ ppm: 7.19–7.25 (m, 3H, CH═CH, CH aromatic), 7.54 (d, 2H, CH aromatic, *J* = 8.0 Hz), 7.72 (t, 1H, CH aromatic, *J* = 16.0 Hz), 7.85 (d, 1H, CH aromatic, *J* = 8.0 Hz), 7.94 (d, 2H, CH aromatic, *J* = 8.4 Hz), 8.02–8.09 (m, 2H, CH═CH, CH aromatic), 8.14 (d, 1H, CH aromatic, *J* = 8.0 Hz), 8.30 (d, 2H, CH aromatic, *J* = 8.0 Hz), 12.44 (s, 1H, NH, exch. D_2O). ^{13}C NMR δ ppm: 116.86, 124.69, 125.89, 126.39, 127.21, 127.80, 129.11, 131.12, 135.11, 136.26, 141.95, 148.04, 151.26, 162.09 (aromatic Cs), 121.76, 134.04 (2 olefinic Cs). Mass (*m/z*): 402 (M+, 5.96), 293 (100). Anal. Calcd for $C_{22}H1_5ClN_4O_2$ (402.38): C, 65.59; H, 3.75; N, 13.91. Found: C, 65.31; H, 3.98; N, 4.25%.

*5.1.5.4. (E)-N-(4-Chlorophenyl)-2-(4-dimethylaminostyryl)quinazolin-4-amine **(12d)**.* Yield 62%; mp 275–277 °C. IR (ν_{max}/cm^{-1}): 3479 (NH), 3055, 2931 (CH aromatic, CH aliphatic). ^{1}H NMR δ ppm: 2.85 (s, 6H, $2CH_3$), 6.55 (d, 2H, CH aromatic, *J* = 8.8 Hz), 6.63 (d, 1H, CH═CH, *J* = 12.0 Hz), 6.67 (d, 2H, CH aromatic, *J* = 8.8 Hz), 7.04 (d, 2H, CH aromatic, *J* = 8.4 Hz), 7.15 (d, 2H, CH aromatic, *J* = 8.4 Hz), 7.44 (t, 1H, CH aromatic, *J* = 14.8 Hz), 7.57 (d, 1H, CH aromatic, *J* = 7.6 Hz), 7.68 (d, 1H, CH═CH, *J* = 16.0 Hz), 7.75 (t, 1H, CH aromatic, *J* = 14.8 Hz), 8.07 (d, 1H, CH aromatic, *J* = 8.0 Hz), 9.68 (s, 1H, NH, exch. D_2O).^{13}C NMR δ ppm: 30.77 (2CH3), 112.90, 114.65, 115.02, 119.45, 119.84, 120.82, 126.02, 126.99, 128.41, 128.73, 129.10, 131.80, 142.80, 149.33, 161.77, 163.12 (aromatic carbons), 121.48, 134.22 (2 olefinic Cs). Mass (*m/z*): 401 (M^+, 16.0), 134 (100). Anal. Calcd for $C_{24}H_{21}ClN_4$ (400.90): C, 71.90; H, 5.28; N, 13.98. Found: C, 71.76; H, 5.49; N, 13.71%.

*5.1.5.5. (E)-4-(2-(4-((4-Chlorophenyl)amino)quinazolin-2-yl)vinyl)-2-methoxyphenol **(12e)**.* Yield 58%; mp 204–206 °C. IR (ν_{max}/cm^{-1}): 3402, 3271 (NH, OH), 3127, 2924 (CH aromatic, CH aliphatic). ^{1}H NMR δ ppm: 3.67 (s, 3H, OCH_3), 4.43 (s, 1H, OH, exch. D_2O), 6.24 (d, 2H, CH aromatic, *J* = 8.0 Hz), 6.55 (d, 1H, CH aromatic, *J* = 8.0 Hz), 6.67 (d, 1H, CH aromatic, *J* = 8.0 Hz), 6.89 (s, 1H, CH aromatic), 7.02 (d, 1H, CH═CH, *J* = 16.0 Hz), 7.10 (d, 2H, CH aromatic, *J* = 8.0 Hz), 7.40–7.43 (m, 2H, CH aromatic, CH═CH), 7.52 (d, 1H, CH aromatic, *J* = 8.0 Hz), 7.71 (t, 1H, CH aromatic, *J* = 15.2 Hz), 8.06 (d, 1H, CH aromatic, *J* = 8.0 Hz), 9.28 (s, 1H, NH, exch. D_2O).^{13}C NMR δ ppm: 55.04 (OCH_3), 107.78, 114.34, 115.69, 117.58, 118.69, 125.86, 126.15, 126.70, 127.21, 128.94, 131.10, 149.64, 151.66, 156.19, 163.56, 170.12, 186.92 (aromatic Cs), 121.04, 134.31 (2 olefinic Cs). Mass (*m/z*): 404 (M^+, 15.1), 151 (100). Anal. Calcd for $C_{23}H_{18}ClN_3O_2$ (403.86): C, 68.40; H, 4.49; N, 10.40. Found: C, 68.53; H, 4.62; N, 10.73%.

*5.1.6. Synthesis of N-(5-methylisoxazol-3-yl) −4- ((2-methylquinazolin-4-yl) amino) benzenesulfonamide **(14)***

A mixture of 4-chloro-2-methylquinazoline **9** (0.89 g, 10 mmole) and sulfamethoxazole (0.56 g, 10 mmole) was refluxed in ethanol (10 mL) in presence of anhydrous potassium carbonate (1.38 g, 10 mmole) for 24 h. The reaction mixture was then cooled, poured onto ice/water and acidified with acetic acid (pH 6). The resulting precipitate was filtered, washed with water, dried and re-crystallized from ethanol. Yield 72%; mp 237–239 °C. IR (ν_{max}/cm^{-1}): 3468, 3394 (NHs), 3066, 2981(CH aromatic, CH aliphatic), 1465, 1138 (SO_2). ^{1}H NMR δ ppm: 2.26 (s, 3H, $\underline{CH_3}$-CO), 2.36 (s, 3H, CH_3), 6.04 (s, 1H, CH aromatic), 6.56 (d, 2H, CH aromatic, *J* = 8.4 Hz), 7.44–7.59 (m, 3H, CH aromatic), 7.57 (d, 1H, CH aromatic, *J* = 8.0 Hz), 7.76 (t, 1H, CH aromatic, *J* = 16.0 Hz), 8.07 (d, 1H, CH aromatic, *J* = 8.00 Hz), 12.26 (s, 1H, NH, exch. D_2O). Mass (*m/z*): 395 (M^+, 1.8), 92 (100). Anal. Calcd for $C_{19}H_{17}N_5O_3S$ (395.43): C, 57.71; H, 4.33; N, 17.71. Found: C, 58.04; H, 4.57; N, 17.62%.

*5.1.7. General procedure for the synthesis of compounds **(15a-d)***

The appropriate aldehyde (20 mmole) was added to a solution of N-(5-methylisoxazol-3-yl)-4-((2-methylquinazolin-4-yl)amino) benzenesulfonamide **14** (3.9 g, 10 mmole) in glacial acetic acid (10 mL) in presence of sodium acetate (1.6 g, 20 mmole). The reaction mixture was refluxed for 24 h. The product was then poured onto ice/water, filtered off, dried and re-crystallized from ethanol to give the desired compound.

*5.1.7.1. (E)-4- ((2-(4-Hydroxystyryl) quinazolin −4- yl) amino) –N- (5-methylisoxazol −3- yl) benzenesulfonamide **(15a)**.* Yield 64%; mp 283–285 °C. IR (ν_{max}/cm^{-1}): 3468, 3332 (NHs, OH), 3066, 2924(CH aromatic, CH aliphatic), 1465, 1126 (SO_2).^{1}H NMR δ ppm: 2.36 (s, 3H, CH_3), 6.08 (s, 1H, CH aromatic), 6.58 (d, 2H, CH aromatic, *J* = 8.8 Hz), 6.83 (d, 1H, CH═CH, *J* = 12.8 Hz), 6.93 (d, 2H, CH aromatic, *J* = 8.4 Hz), 7.12 (s, 1H, OH, exch. D_2O), 7.44–7.52 (m, 3H, CH aromatic), 7.57 (d, 1H, CH aromatic, *J* = 7.6 Hz), 7.62 (t, 1H, CH aromatic, *J* = 10.8 Hz), 7.76 (d, 2H, CH aromatic, *J* = 8.4 Hz), 7.86 (d, 1H, CH═CH, *J* = 14.4 Hz), 8.07 (d, 1H, CH aromatic, *J* = 7.2 Hz), 9.33, 9.79 (s, 2H, 2NH, exch. D_2O). ^{13}C NMR δ ppm: 12.50 (CH_3), 95.74, 113.05, 115.60, 115.90, 116.32, 123.14, 123.52, 126.15, 126.31, 128.88, 129.02, 129.25, 130.95, 142.89, 158.56, 163.83, 170.25, 191.41 (aromatic Cs), 120.67, 132.58 (2 olefinic Cs). Mass (*m/z*): 500 (M^+, 11.5), 57 (100). Anal. Calcd for $C_{26}H_{21}N_5O_4S$ (499.54): C, 62.51; H, 4.24; N, 14.02. Found: C, 62.83; H, 4.51; N, 14.13%.

*5.1.7.2. (E)-4- ((2-(4- Chlorostyryl) quinazolin- 4-yl) amino) -N- (5-methylisoxazol-3- yl) benzenesulfonamide **(15b)**.* Yield 62%; mp 290–292 °C. IR (νmax/cm-1): 3464, 3179 (NHs), 3061, 2920 (CH aromatic, CH aliphatic), 1404, 1118 (SO2).^{1}H NMR δ ppm: 2.30 (s, 3H, CH3), 6.12 (s, 1H, CH aromatic isoxazole), 6.58 (d, 2H, CH aromatic, *J* = 8.4 Hz), 7.01 (d, 1H, CH═CH, *J* = 16.4 Hz), 7.46 (d, 2H, CH aromatic, *J* = 8.4 Hz), 7.50 (m, 3H, CH aromatic), 7.69 (m, 3H, CH aromatic), 7.80 (t, 1H, CH aromatic, *J* = 14.8 Hz), 7.92 (d, 1H, CH═CH, *J* = 16.0 Hz), 8.11 (d, 1H, CH aromatic, *J* = 7.6 Hz), 10.95, 12.38 (s, 2H, 2NH, exch. D2O). ^{13}C NMR δ ppm: 12.53 (CH3), 98.80, 113.49, 115.77, 116.10, 116.53, 123.04, 125.82, 126.35, 126.55, 127.46, 129.56, 129.73, 130.96, 134.75, 137.02, 149.52, 154.41, 162.81, 175.42 (aromatic Cs), 121.67, 134.55 (2 olefinic Cs). Mass (*m/z*): 518 (M+, 36.72), 144 (100). Anal. Calcd for $C_{26}H_{20}ClN_5O_3S$ (517.99): C, 60.29; H, 3.89; N, 13.52. Found: C, 60.18; H, 4.17; N, 13.41%.

*5.1.7.3. (E)-N- (5-Methylisoxazol −3-yl) -((2 -(4- nitrostyryl) quinazolin-4- yl) amino) benzenesulfonamide **(15c)**.* Yield 60%; mp 320–322 °C. IR (ν_{max}/cm^{-1}): 3479, 3178 (NHs), 3055, 2924 (CH aromatic, CH aliphatic), 1512, 1103 (SO2). ^{1}H NMR δ ppm: 2.35 (s, 3H, CH_3), 5.33 (s, 1H, CH aromatic), 7.18 (d, 1H, CH═CH, *J* = 16.0 Hz), 7.49 (d, 2H, CH aromatic, *J* = 6.4 Hz), 7.62 (d, 1H, CH aromatic, *J* = 7.2 Hz), 7.71 (d, 2H, CH aromatic, *J* = 7.2 Hz), 7.79 (t, 1H, CH aromatic, *J* = 15.2 Hz), 7.91 (d, 1H, CH aromatic, *J* = 8.4 Hz), 8.01 (d, 1H, CH═CH, *J* = 16.0 Hz), 8.09 (t, 1H, CH aromatic, *J* = 16 Hz), 8.21 (d, 1H, CH aromatic, *J* = 8.4 Hz), 8.27 (d, 2H, CH aromatic, *J* = 8.4 Hz), 10.15 (s, 1H, NH, exch. D_2O). ^{13}C NMR δ ppm: 12.55 (CH3), 95.37, 113.59, 114.33, 116.00, 116.38, 119.08, 124.29, 125.33, 126.00, 126.66, 127.36, 129.10, 133.55, 135.65, 141.45, 146.26, 147.99, 151.46, 166.87 (aromatic Cs), 122.25, 134.60 (2 olefinic Cs). Mass (*m/z*): 529 (M+, 3.26), 90 (100). Anal. Calcd for $C_{26}H_{20}N_6O_5S$ (528.54): C, 59.08; H, 3.81; N, 15.90. Found: C, 59.27; H, 4.03; N, 16.14%.

*5.1.7.4. (E)-4-((2-(4-Hydroxy-3-methoxystyryl)quinazolin-4-yl)amino)-N-(5-methylisoxazol-3-yl)benzenesulfonamide **(15d)**.* Yield 58%; mp 345–347 °C. IR (ν_{max}/cm^{-1}): 3417, 3332 (NHs, OH), 3066, 2962(CH aromatic, CH aliphatic), 1465, 1126 (SO_2). ^{1}H NMR δ ppm: 2.30 (s, 3H, CH_3), 3.82 (s, 3H, OCH_3), 6.11 (s, 1H, CH aromatic), 6.60 (m, 3H, CH aromatic), 6.86 (d, 1H, CH═CH, *J* = 16.0 Hz), 7.04 (d, 1H, CH aromatic, *J* = 8.0 Hz), 7.40–7.49 (m, 3H, CH aromatic), 7.59–7.65 (m, 2H, CH aromatic), 7.80 (t, 1H, CH aromatic, *J* = 15.2 Hz), 7.91 (d, 1H, CH═CH, *J* = 16.0 Hz), 8.12 (d, 1H, CH aromatic, *J* = 8.0 Hz), 10.96 (s, 1H, NH,

exch. D_2O), 12.29 (s, 1H, OH, exch. D_2O). ^{13}C NMR δ ppm: 12.52 (CH3), 55.79 (OCH3), 95.76, 113.05, 113.91, 115.04, 118.89, 124.59, 126.34, 126.44, 127.49, 128.06, 129.30, 129.79, 132.62, 138.55, 149.62, 152.22, 153.75, 158.46, 161.12, 162.27, 170.31 (aromatic carbons), 121.42, 134.98 (olefinic Cs). Mass (*m/z*): 529 (M^+, 10.5), 43 (100). Anal. Calcd for $C_{27}H_{23}N_5O_5S$ (529.27): C, 61.24; H, 4.38; N, 13.22. Found: C, 60.98; H, 4.50; N, 13.45%.

5.2. In vitro cytotoxic screening

All of the synthesized quinazoline derivatives were chosen for *in vitro* anti-proliferative screening at single concentration of 10 mM for approximately 60 human tumor cell lines panel derived from nine neoplastic diseases (lung, blood, CNS, colon, skin, kidney, ovary, prostate and breast) at the U.S. National Cancer Institute. The detailed procedure of the NCI anticancer screening has been described **(Supplementary M)** according to the reference article [33-35]. Briefly, human tumor cells are inoculated into 96 well microtiter plates in 100 μL at plating densities ranging from 5000 to 40,000 cells/well depending on the doubling time of individual cell lines. After cell inoculation, the microtiter plates are incubated for 24 h prior to addition of experimental drugs. After 24 h, two plates of each cell line are fixed *in situ* with trichloroacetic acid (TCA). Experimental drugs are solubilized in dimethyl sulfoxide and at the time of addition, an aliquot of frozen concentrate is thawed and diluted to twice the desired final maximum test concentration with complete medium containing 50 μg/mL gentamicin. Additional four, 10-fold or ½ log serial dilutions are made to provide a total of five drug concentrations plus control. Aliquots of these different drug dilutions are added to the appropriate microtiter wells already containing 100 μL of medium, resulting in the required final drug concentrations. Following drug addition, the plates are incubated for an additional 48 h. For adherent cells, the assay is terminated by the addition of cold TCA. Cells are fixed *in situ* by the gentle addition of 50 μL of cold 50% (w/v) TCA (final concentration, 10% TCA) and incubated for 60 min at 4 °C. The supernatant is discarded, and the plates are washed five times with tap water and air dried. Sulforhodamine B (SRB) solution is added to each well, and plates are incubated for 10 min at room temperature. After staining, unbound dye is removed and the plates are air dried. Bound stain is subsequently solubilized with 10 mM trizma base, and the absorbance is read on an automated plate reader at a wavelength of 515 nm. For suspension cells, the methodology is the same except that the assay is terminated by fixing settled cells at the bottom of the wells by gently adding 50 μL of 80% TCA (final concentration, 16% TCA). Using the seven absorbance measurements [time zero, (Tz), control growth, (C), and test growth in the presence of drug at the five concentration levels (Ti)], the percentage growth is calculated at each of the drug concentrations levels followed by growth inhibition of 50% (GI_{50}) calculation. The drug concentration resulting in total growth inhibition (TGI). Values are calculated for each of the three parameters if the level of activity is reached; however, if the effect is not reached or is exceeded, the value for that parameter is expressed as greater or less than the maximum or minimum concentration tested.

5.3. Cytotoxicity potential assay study (MTT assay)

The most active compounds (**7a, 7b, 8c, 8e, 12e** and **15b**) were further tested for cytotoxicity on non-small lung cancer cell line (A549) and normal lung fibroblasts (WI38), obtained from the American Type Culture Collection (Rockville, MD, USA) at confirmatory diagnostic unit in VACSERA-Egypt for IC_{50} determination. The detailed procedure was explained (**Supplementary M),** according to Mosmann methodology [36]. Briefly, tumor cells were cultured and then plated in a volume of 100 μL, growth medium + 100 ul of the tested compound per well in a 96-well plate were completed for 24 h before the MTT (3-(4,5-dimethylthiazol-2-yl)-2,5-diphenyltetrazolium bromide) assay. Then, various concentration of test compounds (0.39, 1.56, 6.25, 25 and 100 μg) and the standard reference drug (Lapatinib) were added to the cells. The control cells without the test compounds were also cultured, then the plate was incubated. Cells survival was evaluated at the end of the incubation period via MTT colorimetric assay. After incubation, media were removed and each vial of MTT [M-5655] were reconstituted to be used with 3 mL of medium or balanced salt solution without phenol red and serum. Reconstituted MTT was added in an amount equal to 10% of the culture medium volume and incubated for an additional 4 h. The crystals of formazan were dissolved by adding an amount of MTT Solubilization Solution [M-8910] and the optical density was measured spectrophotometrically at 570 nm. The experiments were performed in three replicates for each concentration of compound; the results were normalized to the control value and expressed as percentage of control. The compound concentrations which give 50% growth inhibition are referred to as the IC_{50}.

Cell viability (% of control) = Absorbance of test - Absorbance of medium × 100/ Absorbance of control

5.4. Epidermal growth factor receptor enzyme inhibition assay

5.4.1. In vitro EGFR enzyme inhibition assay

The *in vitro* EGFR enzyme inhibition assay was performed at confirmatory diagnostic unit, VACSERA, Egypt for selected compounds (**7a, 7b, 8c, 8e, 12e** and **15b**). The evaluation was carried out by ELISA assay method using EnzyChromTM Kinase Assay Kit (EKIN-400) with lapatinib as a reference drug [36,37].

5.4.2. In vitro EGFR enzyme inhibition assay of target compounds against EGFR-expressed in A549 cell line

The assay was carried out according to ELISA assay using Human Bax ELISA (EIA-4487) kits at confirmatory diagnostic unit at VACSERA. Briefly, A549 cell line was incubated with IC_{50} of each compound for 2 h then EGFR concentration and the concentration of each sample was determined by comparing the optical density of the samples to the standard curve using lapatinib as a reference drug; the exact methodology was mentioned in **supplementary M** [37].

5.5. Cellular mechanism of action study

5.5.1. Cell cycle analysis

Cell cycle analysis was carried out for the most active compound **8c** at confirmatory diagnostic unit at VACSERA using Propidium Iodide kit and analyzed by flow cytometry technique. A549 cell line was treated with tested compounds with their IC_{50} for 24 h, then washed, collected by centrifugation, suspended with RNase, stained with (PI) and analyzed by flow cytometry using FACS Calibur reader, compared to the control (cell line without drug treatment) [38].

5.5.2. Cell apoptosis assay

Apoptosis assay was consequently carried out at confirmatory diagnostic unit at VACSERA using Annexin V-FITC Apoptosis detection kit. A biparametric cytofluorimetric analysis was performed using Propidium iodide (PI), which stains DNA and enters only dead cells and fluorescent immunolabeling of the protein annexin-V, which binds to phosphatidylserine (PS) expressed on the surface of the apoptotic cells and fluoresces green after interacting with the labeled annexin-V. In brief, A549 was treated with tested compounds at their IC_{50}, incubated for 24 h, collected, washed with cold PBS, then stained with 5 μL of Annexin V-FITC and 5 μL of propidium iodide, incubated at room temperature for 5 min and finally analyzed by flow cytometry using FACS Caliber detector [39].

5.5.3. Active Caspase-3 expression level assay

To assess caspase-3 activity, the manufacturer's instructions for the human active caspase-3 content assay kit (**supplementary M)** were followed carefully at confirmatory diagnostic unit at VACSERA through

injection of cells with IC_{50} of tested compound **8c** using ROBONIK P2000 ELISA reader [40]. In brief outlined, cells were treated with compound **8c** at its IC50 in 100 µL sample volume per well and incubated for 48 h prior to the assay. Antibody solution was added to each well, incubated for 1 h at R.T. Working Solution was added to each well, incubated 30 min at R.T. The absorbance of each well was measured at 450 nm using ROBONIK P2000 ELISA reader and finally the results were obtained from standard curve using curve fitting software.

5.6. ADMET studies

Computational study for predicted pharmacokinetic properties and toxicity of the target compounds **7a, 7b, 8c, 8e, 12b** and **15d** have been performed based on their ADMET (absorption, distribution, metabolism, elimination, and toxicity) profiles and results were presented in Tables 7-11. The ADMET studies were predicted using pkCSM tool (http://biosig.unimelb.edu.au/pkcsm/prediction) [41]. The SMILE molecular structures of the compounds were obtained from PubChem (https://pubchem.ncbi.nlm.nih.gov).

5.7. Molecular docking study

All molecular modeling calculations and docking studies were performed using "Molecular Operating Environment (MOE) version 2019.0101' software (MOE of Chemical Computing Group Inc., on a Core i5 2.2 GHz workstation) running on a Windows 10 PC. The target compounds **7a, 7b, 8c, 8e, 12e** and **15b** were built in MOE. The X-ray crystallographic structure of EGFR kinase enzyme complexed with reference drug lapatinib [43] (PDB ID: 1XKK) was obtained from the protein data bank (http://www.rcsb.org/). Enzyme preparation was carried out by removing the co-crystallized ligand, sodium ion and water molecules, then quick preparation protocol in MOE with default options was used. To ensure the validity of the docking protocol, re-docking of the native lapatinib into the active site was performed. Preparation of the target compounds for docking was carried out by drawing 2D structures using Marvin Sketch, 3D protonation of the structure, running conformational analysis using systemic search and finally selecting the least energetic conformer. Poses were scored by initial rescoring methodology (GBVI/WSA dg) and the final rescoring methodology (GBVI/WSA dg) and the best scoring pose was determined. Receptor-ligand interactions were showed in 2D and 3D styles.

Declaration of Competing Interest

The authors declare that they have no known competing financial interests or personal relationships that could have appeared to influence the work reported in this paper.

Acknowledgment

The authors are thankful to the *National Cancer Institute (NCI),* staff for performing the in vitro anticancer testing for all synthesized compounds over their panel of cell lines.

Funding Sources

This research did not receive any specific grant from funding agencies in the public, commercial, or not-for-profit sectors.

Appendix A. Supplementary material

Supplementary data to this article can be found online at https://doi.org/10.1016/j.bioorg.2020.104358.

References

[1] A. Irfan, F. Batool, S.A.Z. Naqvi, A. Islam, S.M. Osman, A. Nocentini, S.A. Alissa, C. T. Supuran, Benzothiazole derivatives as anticancer agents, J. Enzym. Inhib. Med. Ch. 35 (1) (2020) 265–279, https://doi.org/10.1080/14756366.2019.1698036.

[2] M.C. Egbujor, U.C. Okoro, New Methionine-based P-toluenesulphonamoyl carboxamide derivatives as antimicrobial and antioxidant agents: design, synthesis and molecular docking, J. Pharm. Res. Int. 28 (1) (2019) 1–12, https://doi.org/10.9734/jpri/2019/v28i130192.

[3] G.S. Karagiannis, J.S. Condeelis, M.H. Oktay, Chemotherapy-induced metastasis: molecular mechanisms, clinical manifestations, therapeutic interventions, Cancer Res. 79 (18) (2019) 4567–4576, https://doi.org/10.1158/0008-5472.CAN-19-1147.

[4] Hai-Q. Zhang, Fei-H. Gong, Ji-Q. Ye, C. Zhang, Xiao-H. Yue, Chuan-G. Li, Yun-G. Xu, Li-P. Sun, Design and discovery of 4-anilinoquinazoline-urea derivatives as dual TK inhibitors of EGFR and VEGFR-2, Eur. J. Med. Chem. 125 (2017) 245-254. doi: 10.1016/j.ejmech.2016.09.039.

[5] D. Das, L. Xie, J. Wang, X. Xu, Z. Zhang, J. Shi, X. Le, J. Hong, Discovery of new quinazoline derivatives as irreversible dual EGFR/HER2 inhibitors and their anticancer activities – Part 1, Bioorg. Med. Chem. Letters. 29 (4) (2019) 591–596, https://doi.org/10.1016/j.bmcl.2018.12.056.

[6] D. Das, J. Hong, Recent advancements of 4-aminoquinazoline derivatives as kinase inhibitors and their applications in medicinal chemistry, Eur. J. Med. Chem. 170 (2019) 55–72, https://doi.org/10.1016/j.ejmech.2019.03.004.

[7] H.A.M. El-Sherief, B.G.M. Youssif, S.N.A. Bukhari, A.H. Abdelazeem, M. Abdel-Aziz, H.M. Abdel-Rahman, Synthesis, anticancer activity and molecular modeling studies of 1,2,4-triazole derivatives as EGFR inhibitors, Eur. J. Med. Chem. 156 (2018) 774–789, https://doi.org/10.1016/j.ejmech.2018.07.024.

[8] W. Hou, Y. Ren, Z. Zhang, H. Sun, Y. Ma, B. Yan, Novel quinazoline derivatives bearing various 6-benzamide moieties as highly selective and potent EGFR inhibitors, Bioorg. Med. Chem. 26 (8) (2018) 1740–1750, https://doi.org/10.1016/j.bmc.2018.02.022.

[9] K. Yang, X. Ren, L. Tao, P. Wang, H. Jiang, L. Shen, Y. Zhao, Y. Cui, M. Li, Song Lin, Prognostic implications of epidermal growth factor receptor variant III expression and nuclear translocation in Chinese human gliomas, Chin. J. Cancer Res. 31 (1) (2019) 188–202, https://doi.org/10.21147/j.issn.1000-9604.2019.01.14.

[10] B. Jutten, T.G. Keulers, H.J.M. Peeters, M.B.E. Schaaf, K.G.M. Savelkouls, I. Compter, R. Clarijs, O.E.M.G. Schijns, L. Ackermans, O.P.M. Teernstra, M. I. Zonneveld, R.M.E. Colaris, L. Dubois, M.A. Vooijs, J. Bussink, J. Sotelo, J. Theys, G. Lammering, K.M.A. Rouschop, EGFRvIII expression triggers a metabolic dependency and therapeutic vulnerability sensitive to autophagy inhibition, Autophagy. 14 (2) (2018) 283–295, https://doi.org/10.1080/15548627.2017.1409926.

[11] K. Abouzid, S. Shouma, Design synthesis and in vitro antitumor activity of 4-aminoquinoline and 4-aminoquinazoline derivatives targeting EGRF tyrosine kinase, Bioorg. Med. Chem. 16 (2008) 7543–7551, https://doi.org/10.1016/j.bmc.2008.07.038.

[12] H.A.A. Allam, E.E. Aly, A.K.B.A.W. Farouk, A. Elkerdawy, E. Rashwan, S.E. S. Abbass, Design and Synthesis of some new 2,4,6-trisubstituted quinazoline EGFR inhibitors as targeted anticancer agents, Bioorg. Chem. 98 (2020), 103726, https://doi.org/10.1016/j.bioorg.2020.103726.

[13] D. Das, J. Hon, Recent advancements of 4-aminoquinazoline derivatives as kinase inhibitors and their applications in medicinal chemistry, Eur. J. Med. Chem. 170 (2019) 55–72, https://doi.org/10.1016/j.ejmech.2019.03.004.

[14] Z. Faghih, N. Rahmannejadi, R. Sabet, K. Zomorodian, M. Asad, S. Khabnadideh, Synthesis of some novel dibromo-2-arylquinazolinone derivatives as cytotoxic agents, Res Pharm Sci. 14 (2) (2019) 115–121, https://doi.org/10.4103/1735-5362.253358.

[15] V. Alagarsamy, K. Chitra, G. Saravanan, V.R. Solomon, M.T. Sulthana, B. Narendhar, An overview of quinazolines: Pharmacological significance and recent developments, Eur. J. Med. Chem. 151 (2018) 628–685, https://doi.org/10.1016/j.ejmech.2018.03.076.

[16] S. Gatadi, T.V. Lakshmi, S. Nanduri, 4(3H)-Quinazolinone derivatives: Promising antibacterial drug leads, Eur. J. Med. Chem. 170 (2019) 157–172, https://doi.org/10.1016/j.ejmech.2019.03.018.

[17] B. Kapoor, A. Nabi, R. Gupta, M. Gupta, Synthesis and antimicrobial evaluation of quinazolinone peptide derivatives, Asian J. Pharm. Clin. Res. 10 (16) (2017) 7–12, https://doi.org/10.22159/ajpcr.2017.v10s4.21329.

[18] Xiao-F. Shang, S.L. Morris-Natschke, Guan-Z. Yang, Ying-Q. Liu, X. Guo, Xiao-S. Xu, M. Goto, Jun-C. Li, Ji-Y. Zhang, Kuo-H. Lee, Biologically active quinoline and quinazoline alkaloids part II. Med. Res. Rev. 38 (2018) 1614–1660. doi: 10.1002/med.21492.

[19] D. Xie, J. Shi, A. Zhang, Z. Lei, G. Zu, Y. Fu, X. Gan, L. Yin, B. Song, D. Hu, Syntheses, antiviral activities and induced resistance mechanisms of novel quinazoline derivatives containing a dithioacetal moiety, Bioorg. Chem. 80 (2018) 433–443, https://doi.org/10.1016/j.bioorg.2018.06.026.

[20] X. Xia, Y. Liu, Y. Liao, Z. Guo, C. Huang, F. Zhang, L. Jiang, X. Wang, J. Liu, H. Huang, Synergistic effects of gefitinib and thalidomide treatment on EGFR-TKI-sensitive and -resistant NSCLC, Eur. J. Pharmacol. 856 (2019) 1–5, https://doi.org/10.1016/j.ejphar.2019.172409.

[21] X. Qin, Y. Lv, P. Liu, Z. Li, L. Hu, C. Zeng, L. Yang, Novel Morpholin-3-One Fused Quinazoline Derivatives as EGFR Tyrosine Kinase Inhibitors, Bioorg. Med. Chem. Letters 26 (2016) 1571–1575, https://doi.org/10.1016/j.bmcl.2016.02.009.

[22] A.S. El-Azab, A.A.-M. Abdel-Aziz, S. Bua, A. Nocentini, M.A. El-Gendy, M. A. Mohamed, T.Z. Shawer, N.A. AlSaif, C.T. Supuran, Synthesis of benzensulfonamides linked to quinazoline scaffolds as novel carbonic anhydrase

inhibitors, Bioorg. Chem. 87 (2019) 78–90, https://doi.org/10.1016/j.bioorg.2019.03.007.
[23] K.P. Rakesh, S.-M. Wang, J. Leng, L. Ravindar, A.M. Asiri, H.M. Marwani, H.-L. Qin, Recent development of sulfonyl or sulfonamide hybrids as potential anticancer agents: a key review, Anticancer Agents Med. Chem. 18 (4) (2018) 488–505, https://doi.org/10.2174/1871520617666171103140749.
[24] G. Banuppriya, R. Sribalan, V. Padmini, Synthesis and characterization of curcumin-sulfonamide hybrids: Biological evaluation and molecular docking studies, J. Mol. Struct. 1155 (2018) 90–100, https://doi.org/10.1016/j.molstruc.2017.10.097.
[25] M.V. Kachaeva, D.M. Hodyna, I.V. Semenyuta, S.G. Pilyo, V.M. Prokopenko, V. V. Kovalishyn, L.O. Metelytsia, V.S. Brovarets, Design, synthesis and evaluation of novel sulfonamides as potential anticancer agents, Comput. Biol. Chem. 74 (2018) 294–303, https://doi.org/10.1016/j.compbiolchem.2018.04.006.
[26] M. Soliman, A.S. Alqahtani, M.M. Ghorab, Novel sulfonamide benzoquinazolinones as dual EGFR/HER2 inhibitors, apoptosis inducers and radiosensitizers, J. Enzyme Inhib. Med. Chem. 34 (1) (2019) 1030–1040, https://doi.org/10.1080/14756366.2019.1609469.
[27] E. Moreno, D. Plano, I. Lamberto, M. Font, I. Encío, J.A. Palop, C. Sanmartín, Sulfur and selenium derivatives of quinazoline and pyrido[2,3-d]pyrimidine: Synthesis and study of their potential cytotoxic activity in vitro, Eur. J. Med. Chem. 47 (2012) 283–298, https://doi.org/10.1016/j.ejmech.2011.10.056.
[28] A. Mrozek-Wilczkiewicz, E. Spaczynska, K. Malarz, W. Cieslik, M. Rams-Baron, V. Kryštof, R. Musiol, Design, synthesis and in vitro activity of anticancer styrylquinolines. The p53 independent mechanism of action, PLoS ONE 10 (11) (2015), e0142678, https://doi.org/10.1371/journal.pone.0142678.
[29] N. Jiang, X. Zhai, T. Li, D. Liu, T. Zhang, B. Wang, P. Gong, Design, synthesis and antiproliferative activity of novel 2-substituted-4-amino-6-halogenquinolines, Molecules 17 (2012) 5870–5881, https://doi.org/10.3390/molecules17055870.
[30] A.Y.H. Helali, M.T.M. Sarg, M.M.S. Koraa, M.S.F. El-Zoghbi, Utility of 2-methyl-quinazolin-4(3H)-one in the synthesis of heterocyclic compounds with anticancer activity, J. Med. Chem. 4 (2014) 12–37, https://doi.org/10.4236/ojmc.2014.41002.
[31] J. Jampilek, R. Musiol, J. Finster, M. Pesko, J. Carroll, K. Kralova, M. Vejsova, J. O'Mahony, A. Coffey, J. Dohnal, J. Polanski, Investigating biological activity spectrum for novel styrylquinazoline analogues, Molecules 14 (2009) 4246–4265, https://doi.org/10.3390/molecules14104246.
[32] O.M. Antypenko, L.M. Antypenko, S.I. Kovalenko, A.M. Katsev, O.M. Achkasova, Potential of N-aryl(benzyl, heteryl)-2-(tetrazolo[1,5-c]quinazolin-5-ylthio) acetamides as anticancer and antimicrobial agents, Arab. J. Chem. 9 (6) (2016) 792–805, https://doi.org/10.1016/j.arabjc.2014.09.009.
[33] H.S. Ibrahim, M.E. Albakri, W.R. Mahmoud, H.A. Allam, A. Reda, H.A. Abdel-Aziz, Synthesis and biological evaluation of some novel thiobenzimidazole derivatives as anti-renal cancer agents through inhibition of c-MET kinase, Bioorg. Chem. 85 (2019) 337–348, https://doi.org/10.1016/j.bioorg.2019.01.006.
[34] A. Alshammari, A. El-Gazzar, H. Hafez, Efficient synthesis of a new class of N-nucleosides of 4H-thiochromeno[2,3-d]pyrimidine-10-sulfone as potential anticancer and antibacterial agents, Int. J. Org. Chem. 3 (3A) (2013) 15–27, https://doi.org/10.4236/ijoc.2013.33A003.
[35] M. Zusso, V. Lunardi, D. Franceschini, A. Pagetta, R. Lo, S. Stifani, A.C. Frigo, P. Giusti, S. Moro, Ciprofloxacin and levofloxacin attenuate microglia inflammatory response via TLR4/NF-kB pathway, J. Neuroinflammation. 16 (148) (2019), https://doi.org/10.1186/s12974-019-1538-9.
[36] S.Valsalam, P. Agastian, M. V. Arasu, N. A. Al-Dhabi, Abdul-K. M. Ghilan, K. Kaviyarasu, B. Ravindran, S.W. Chang, S. Arokiyaraj, Rapid biosynthesis and characterization of silver nanoparticles from the leaf extract of Tropaeolum majus L. and its enhanced in-vitro antibacterial, antifungal, antioxidant and anticancer properties, J. Photochem. Photobiol. B, Biol. 191 (2019) 65-74. doi: 10.1186/s12974-019-1538-9.
[37] A.A. Mouineer, A.F. Zaher, A.A. El-Malah, E. Sobh, Design, synthesis, antitumor activity, cell cycle analysis and elisa assay for cyclin dependant kinase-2 of a new (4-aryl-6-flouro-4h-benzo[4, 5] thieno[3, 2-b] pyran) derivatives, Mediterr. J. Chem. 6 (5) (2017) 165–179, https://doi.org/10.13171/mjc65/01709262240-zaher.
[38] M. Maher, A.E. Kassab, A.F. Zaher, Z. Mahmoud, Novel pyrazolo[3,4-d] pyrimidines: design, synthesis, anticancer activity, dual EGFR/ErbB2 receptor tyrosine kinases inhibitory activity, effects on cell cycle profile and caspase-3-mediated apoptosis, J Enzyme Inhib. Med. Chem. 34 (1) (2019) 532–546, https://doi.org/10.1080/14756366.2018.1564046.
[39] Ye-J. Kim, T. Tsang, G.R. Anderson, J.M. Posimo, D.C. Brady, Inhibition of BCL2 Family Members Increases the Efficacy of Copper Chelation in BRAFV600E-Driven Melanoma, Cancer Res. 80 (7) (2020) 1387-1400. doi: 10.1158/0008-5472.CAN-19-1784.
[40] K.M. Amin, Y.M. Syam, M.M. Anwar, H.I. Ali, T.M. Abdel-Ghani, A.M. Serry, Synthesis and molecular docking study of new benzofuran and furo[3,2-g] chromone-based cytotoxic agents against breast cancer and p38a MAP kinase inhibitors, Bio. Org. 76 (2018) 487–500, https://doi.org/10.1016/j.bioorg.2017.12.029.
[41] D.E.V. Pires, T.L. Blundell, D.B. Ascher, pkCSM: Predicting Small-Molecule Pharmacokinetic and Toxicity Properties Using Graph-Based Signatures, J. Med. Chem. 58 (9) (2015) 4066–4072, https://doi.org/10.1021/acs.jmedchem.5b00104.
[42] A.O. Adeoye, B.J. Oso, I.F. Olaoye, H. Tijjani, A.I. Adebayo, Repurposing of chloroquine and some clinically approved antiviral drugs as effective therapeutics to prevent cellular entry and replication of coronavirus, J. Biomol. Struct. Dyn. (2020), https://doi.org/10.1080/07391102.2020.1765876.
[43] B.W. Katona, R.A. Glynn, K.E. Paulosky, Z. Feng, C.I. Davis, J. Ma, C.T. Berry, K. M. Szigety, S. Matkar, Y. Liu, H. Wang, Y. Wu, X. He, B.D. Freedman, D.C. Brady, X. Hua, Combined Menin and EGFR Inhibitors Synergize to Suppress Colorectal Cancer via EGFR-Independent and Calcium-Mediated Repression of SKP2 Transcription, Cancer Res. 79 (9) (2019) 2195–2207, https://doi.org/10.1158/0008-5472.CAN-18-2133.